Massachusetts Institute of Technology
Charles Stark Draper Laboratory
Cambridge, Massachusetts

Luminary Memo # 194

TO: Russell Larson
FROM: Allan Klumpp
DATE: January 22, 1971
SUBJECT: Analysis of the Yaw Divergence at P64 Terminus

INTRODUCTION

My memo to you on January 12 (Ref. 1) reported on the results of an examination of several anomalies and stated that analyses would be made and the results published shortly. The analysis of the yaw divergence has been completed and is reported here. Analyses of other anomalies about whose causes I was uncertain in the preceding memo will be completed and reported separately.

This analysis is basedon rollbacks of a single descent simulation. The relative importance of the sources of yaw divergence may be different in other simulations.

SHORT DESCRIPTION OF GUIDANCE AND YAW CONTROL INTERACTION

This is intended to provide enough background information on descent guidance and control to understand what follows. During lunar descent the guidance equations are processed in a "guidance coordinate frame" (see Fig. 1) which rotates with the moon and whose origin is, on each guidance pass, brought into coincidence with the current landing site produced by lunar rotation and landing site redesignations, if any. On a nominal descent, the XG, YG, ZG axes of the guidance coordinate frame are parallel to the XP, YP, ZP axes of the platform frame at the instant of touchdown, but this is true only at that instant because the guidance frame rotates with the moon and the platform frame does not. Figure 1, adapted from Ref. 2, shows the erection of the guidance coordinate frame. TTF is the current time relative to reaching the phase targets (the negative of the time to go) and GAINBRAK = 1 or GAINAPPR = 0 is selected according to phase. Thus during the approach phase the guidance coordinate frame is oriented about the vertical XG axis such that the YG axis is normal to the vertical plane defined by the line of sight to the landing site and the XG axis. The ZG axis is therefore horizontal and roughly forward along the direction of motion.

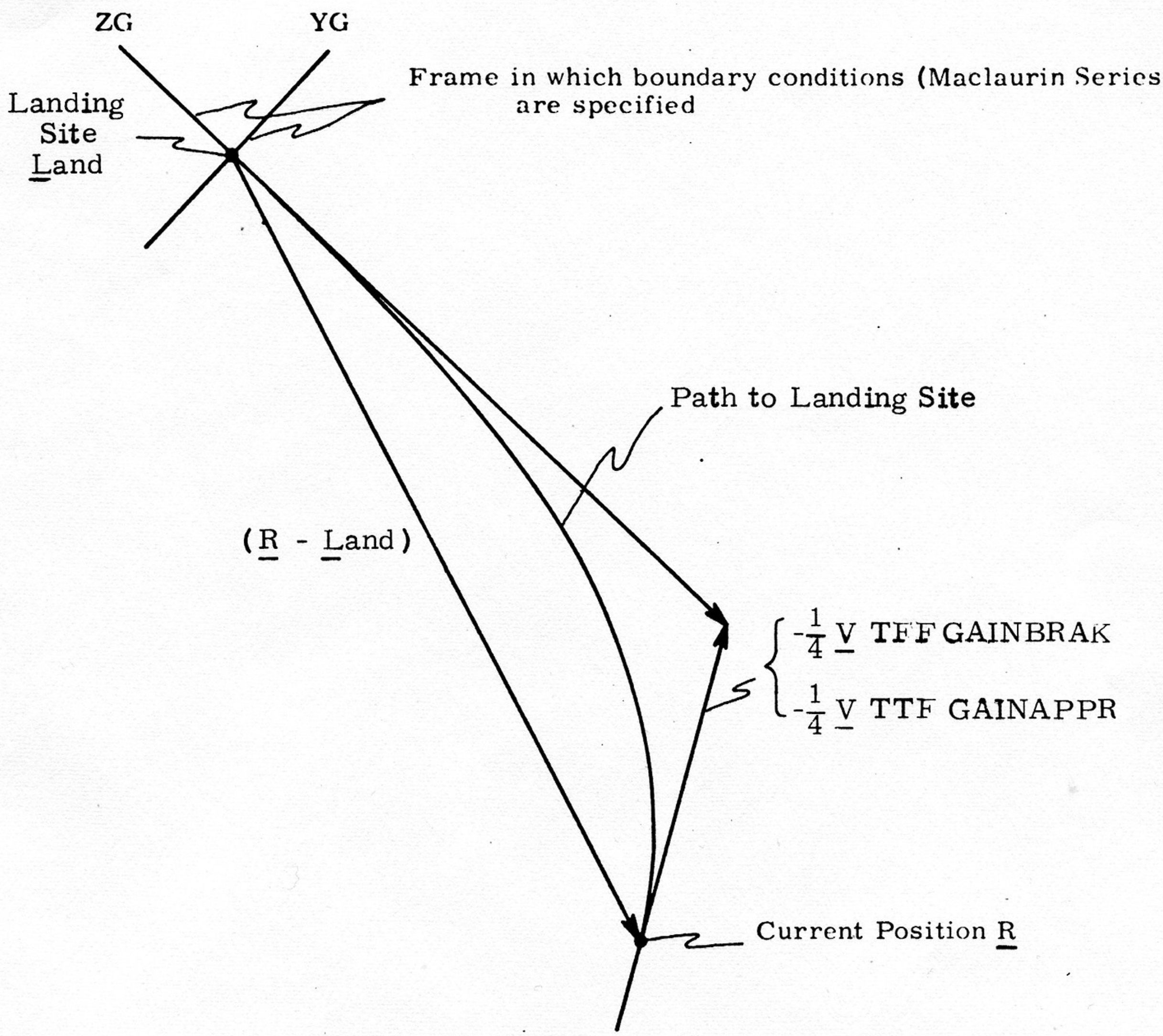

Fig. 1 Plan View Showing Orientation of the Guidance Coordinate Frame.

The guidance equations produce a window pointing command vector $\underline{U}NWC$ for the powered flight attitude maneuver routine FINDCDUW. For most of the approach phase, $\underline{U}NWC$ is merely the line of sight vector to the landing site. The intention is to yaw the LM such that its plane of symmetry — defined by the ZB, XB LM body axes - contains the vector $\underline{U}NWC$. With $\underline{U}NWC$ being the line of sight vector, the landing site will be superimposed upon the LPD reticle. Line-of-sight yaw control works well provided the line of sight is separated from the XB axis by a sufficient angle. Figure 2, adapted from Ref. 2, shows why line-of-sight yaw control cannot be used all the way to the landing site. As the line of sight approaches the XB axis, yaw control becomes indeterminate, and an alternate window pointing command vector must be used. The alternate used is the guidance coordinate frame ZG axis. The criterion for switching between the line-of-sight vector and the ZG axis need not be explained in detail here (see Ref. 2), but for a landing which is approximately planar, the line of sight vector is used exclusively until the LPD angle reaches 65°, the ZG axis is used exclusively beyond 75°, and between 65° and 75° the two vectors are mixed as a linear function of the cosine of the LPD angle.

In a nominal automatic landing, the transition between window pointing command vectors starts about 5 seconds before the end of P64, and will just about be complete on the final P64 pass. Thus the landing site will be kept on the LPD reticle until it disappears out the bottom of the window, and then the LM will yaw slightly to aline the reticle in the direction of the ZG axis. The yaw motion produced by the final P64 command will normally persist into the second pass of P66.

Guidance commands to the powered flight attitude maneuver routine FINDCDUW consist of a thrust pointing command vector $\underline{U}NFC$ and the window pointing command vector $\underline{U}NWC$. Using these two vectors FINDCDUW erects a commanded body axis coordinate frame twice, as shown in Fig. 3, adapted from Ref. 3. The first iteration satisfies the geometry constraints exactly but fails to account for the angular displacement between the thrust vector and the true X body axis. The second iteration corrects for this thrust offset and introduces a small error in window pointing. This window pointing error, defined as the angle between the ZCB XCB plane and the line of sight vector, is the product of the sine of the LPD angle and the thrust offset angle about the ZCB axis. Consequently the window pointing error ranges from zero when the LPD angle is zero, to the thrust offset about Z (whose maximum is under 1°) when the LPD angle is 90°. FINDCDUW does not correct this error.

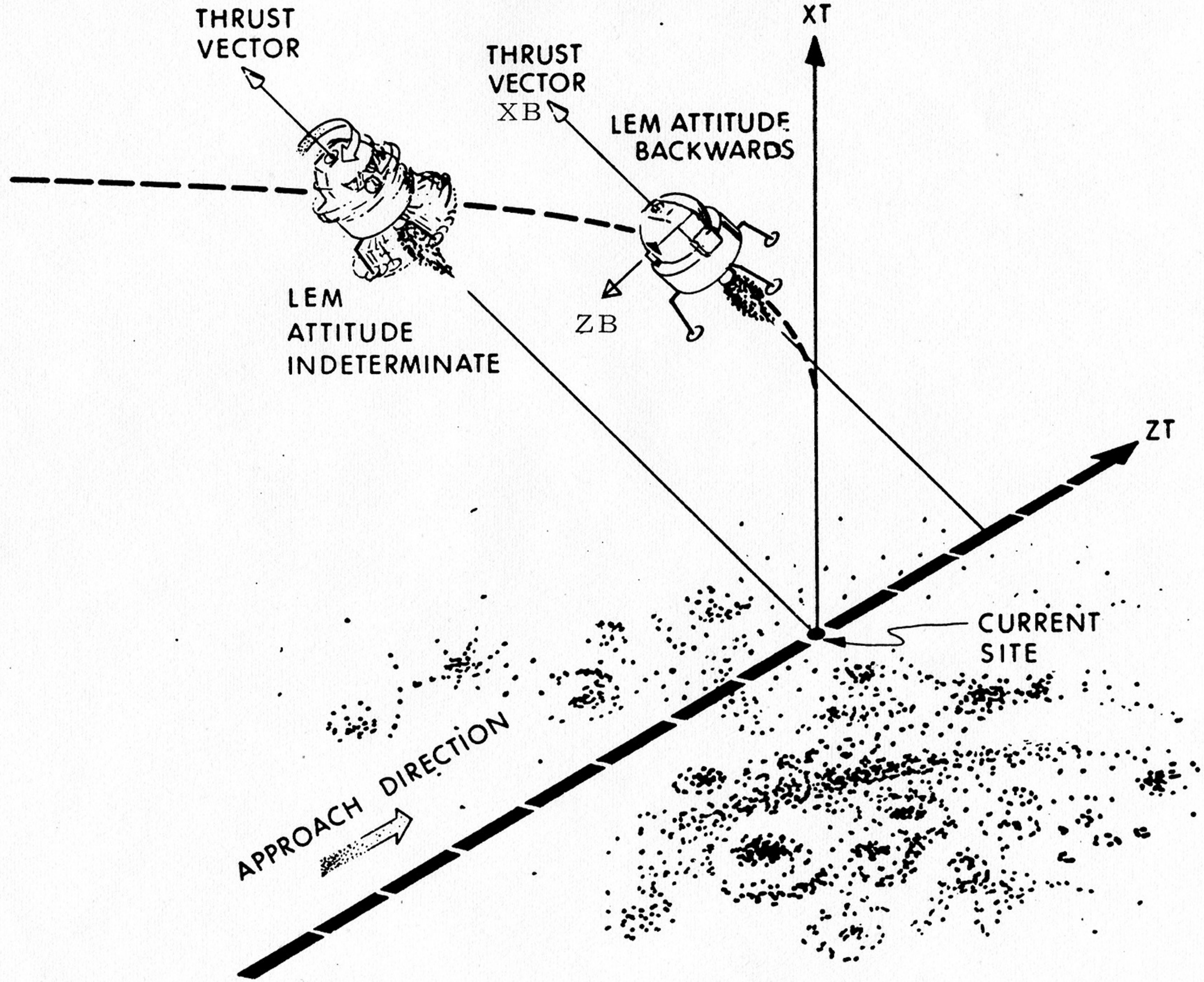

Fig. 2 Why Keeping the Landing Site in the Center of Vision cannot be the Sole Criterion for Controlling Attitude about the Thrust Axis.

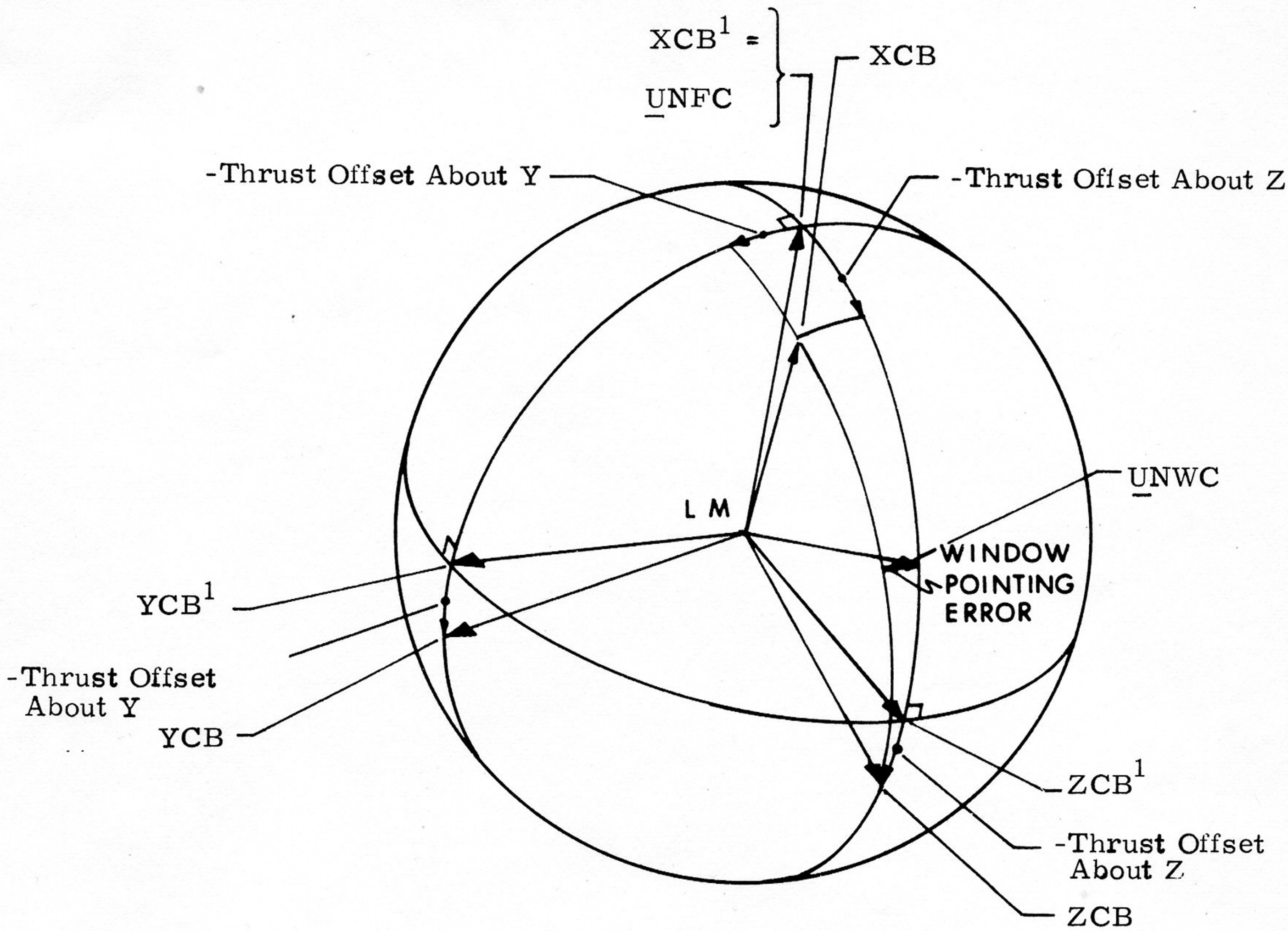

NOTE: **Commanded body axes are computed in two steps.** Vectors computed the first step are identified by the superscript 1. Final values have no superscripts.

Fig. 3 Geometry of Erection of Commanded Body Axes Viewed on a LM Centered Unit Sphere.

Using the commanded body axis coordinate frame of Fig. 3, FINDCDUW computes corresponding commanded gimbal angles to bring the actual body coordinate frame into coincidence with commanded frame. FINDCDUW issues to the digital autopilot gimbal-angle-increment commands that the autopilot uses to increment the desired gimbal angles every tenth of a second during the succeeding two seconds. At the end of the two second period the autopilot's desired gimbal angles coincide with FINDCDUW's commanded gimbal angles of the beginning of the two second period, and FINDCDUW updates the gimbal-angle-increment commands from new information. The digital autopilot closes the attitude control loop driving the actual gimbal angles into close proximity with its desired gimbal angles.

One statement of the preceding memo (Ref. 1) was not correct. The sudden increase in the yaw rate a few seconds prior to P64 was not caused by switching from line-of-sight window pointing to ZG-axis window pointing. The simultaneity of the break point in the yaw profile with the 65° LPD angle was coincidental not causal. The roll angle in the simulation described was caused by thrust offset rather than by an out-of-plane thrust pointing command vector. Because FINDCDUW does not correct yaw for thrust offset, the yaw attitude was not being suppressed by the roll attitude prior to attaining 65° LPD angle as erroneously reported in Ref. 1.

SOURCES OF YAW DIVERGENCE

Four sources of yaw divergence have been found:

1. Out-of-plane velocity due to initial condition dispersions and accelerometer bias eventually detected by the landing radar, or due to azimuth landing site redesignation. This produces a non-planar approach phase trajectory as illustrated in Fig. 1, and the yaw angle acquired is not erroneous but is a normal and desirable feature of a non-planar approach. In the run analyzed, the Y velocity in guidance coordinates at the start of the approach phase was .31 m/s to the right and the guidance frame was rotated 4 mr about the vertical.

2. Truncation of the landing site update by the descent guidance equations. (This source was discovered by Lowell Hull, Ref. 4.) Every guidance pass the landing site is updated in platform coordinates by the equation

$$\underline{LAND} = \underline{LAND}\ \mathrm{UNIT}\,(\underline{LAND} + \underline{W}M \times \underline{LAND}\,\Delta t)$$

where $\underline{W}M$ is the lunar angular rate vector and Δt is the guidance period. With an approach azimuth north of west, the landing site is updated to the right each guidance pass. The updating is truncated to an integer 1/8 m, consequently on every guidance pass there is an apparent landing site redesignation to the left of up to 1/8 m. For a given latitude, the magnitude of this truncation error is a sawtooth function of the cosine of the approach azimuth (defined to the east of north) as illustrated in Fig. 4. The approach azimuth of the Apollo 14 trajectory is 283.7° and produces a truncation error every two seconds of -.059 m, about half of the maximum. With these repeated apparent landing site redesignations to the left, the LM will yaw increasingly to the left, and, regardless of how small the redesignation is, the yaw increment will increase each guidance pass and become unbounded as the LM flies over the site. Of course, P66 begins automatically before this can happen.

3. The digital autopilot is incapable of attaining zero roll error. Consequently any roll error (about the ZB axis) will produce an out-of-plane acceleration error, rotation of the guidance coordinate frame about the vertical, and rotation of the LM in yaw. In simulations, this error has been found small compared to the previous two.

4. A mistake was made twice in the LGC program computations erecting the guidance coordinate frame. (See Ref. 5.) The net result of these mistakes is that, with Apollo 14 erasables, on the final pass of P64 the LGC uses .246155 for GAINAPPR instead of 0. This means that the orientation of the guidance coordinate frame is based on the out-of-plane velocity on the final P64 pass, a violation of the intended procedure. We are favored by chance that this gain constant is small compared to unity.

SIMULATION RESULTS

Simulation results have been analyzed to determine whether or not the sources cited explain all of the yaw observed, and we believe they do. Figure 5, illustrating these results, contains three parts. The upper part shows that the yaw angle and the azimuth angle of the guidance coordinate frame follow very closely, as to be expected. The second part of Fig. 5 shows that the landing site does move precisely 2.125 m each 2 seconds, as predicted. The LM motion is also plotted, and it converges on the landing site motion, as expected.

FOR LANDING SITE RADIUS = 1 738.090

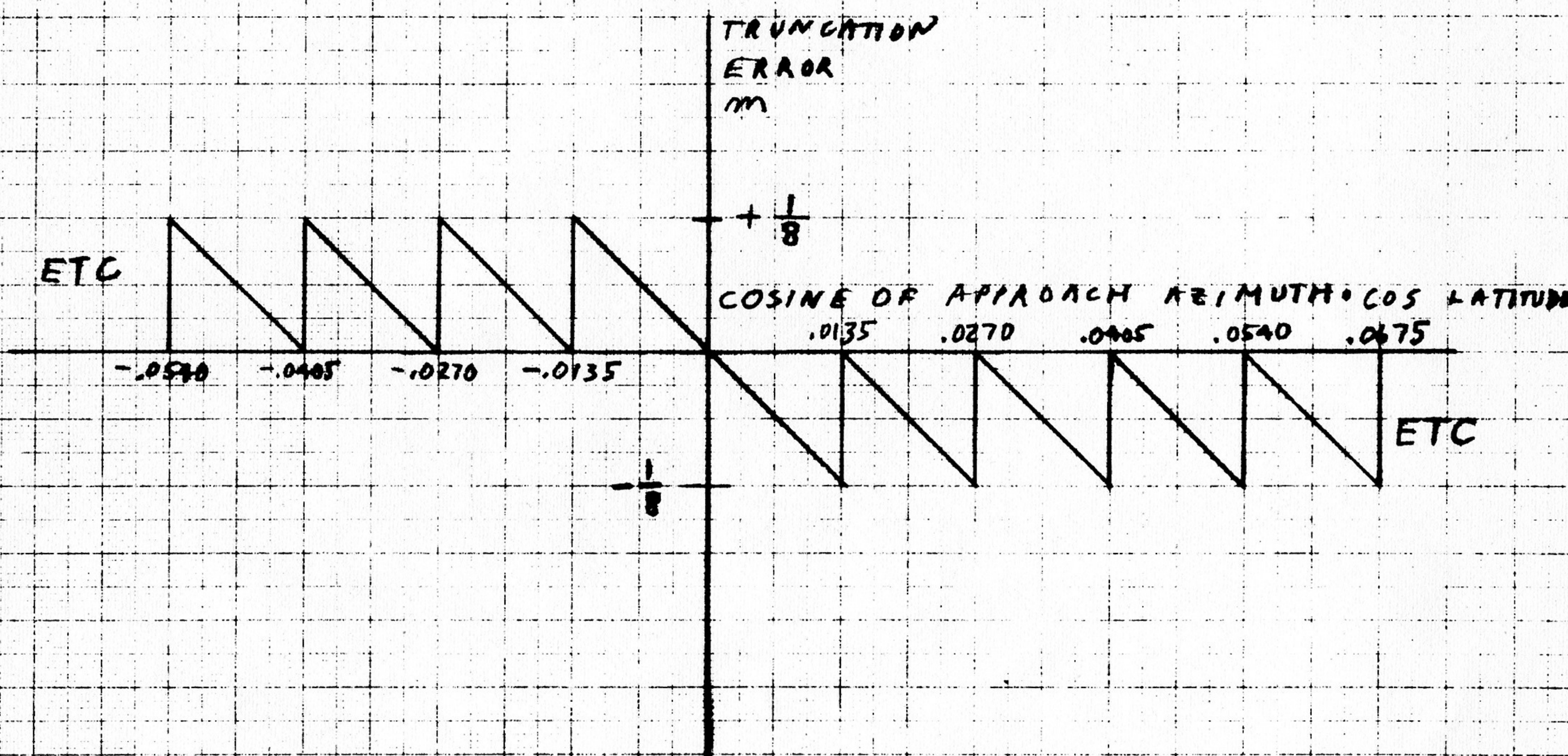

LANDING SITE TRUNCATION ERROR IN THE Y PLATFORM DIRECTION

PER GUIDANCE CYCLE

FIGURE 4

FIGURE 5

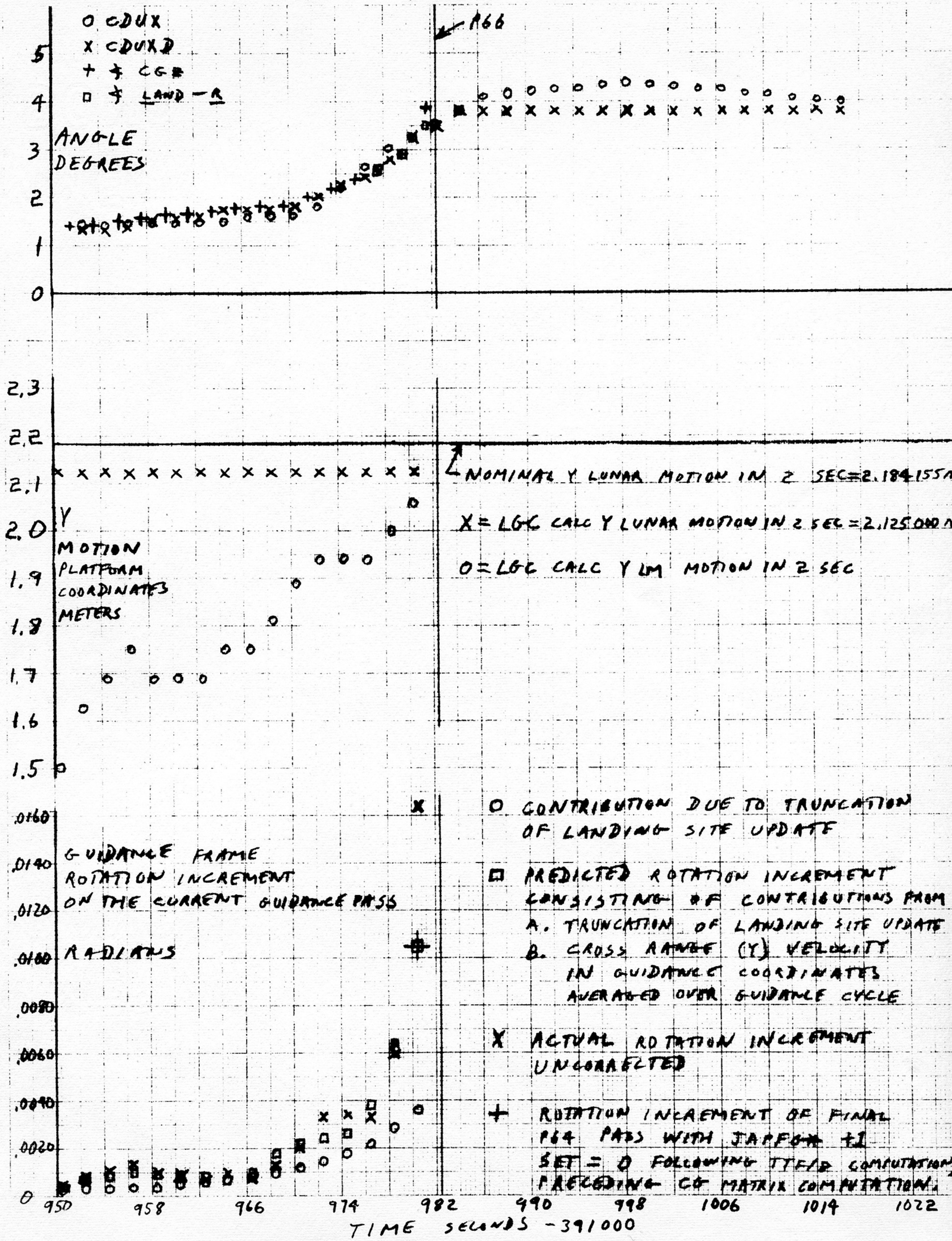

O CDUX
X CDUXD
+ CG
□ LAND - R
P66
ANGLE DEGREES
5
4
3
2
1
0
2.3
2.2
2.1
2.0
1.9
1.8
1.7
1.6
1.5
NOMINAL Y LUNAR MOTION IN 2 SEC=2.184155
X= LGC CALC Y LUNAR MOTION IN 2 SEC = 2.125000
O= LGC CALC Y LM MOTION IN 2 SEC
Y MOTION PLATFORM COORDINATES METERS
.0160
.0140
.0120
.0100
.0080
.0060
.0040
.0020
0
GUIDANCE FRAME ROTATION INCREMENT ON THE CURRENT GUIDANCE PASS
RADIANS
O CONTRIBUTION DUE TO TRUNCATION OF LANDING SITE UPDATE
□ PREDICTED ROTATION INCREMENT CONSISTING OF CONTRIBUTIONS FROM
A. TRUNCATION OF LANDING SITE UPDATE
B. CROSS RANGE (Y) VELOCITY IN GUIDANCE COORDINATES AVERAGED OVER GUIDANCE CYCLE
X ACTUAL ROTATION INCREMENT UNCORRECTED
+ ROTATION INCREMENT OF FINAL P64 PASS WITH JAPFOR +1 SET = 0 FOLLOWING TTF/8 COMPUTATION PRECEDING CG MATRIX COMPUTATION.
950
958
966
974
982
990
998
1006
1014
1022
TIME SECONDS -391000

The most interesting revelation of Fig. 5 is the bottom plot which shows the rotation increment of the guidance coordinate frame on each guidance cycle (X) as compared to a predicted rotation increment (□). The rotation increment is within 1 mr of the prediction every pass except the last P64 pass when the discrepancy is about 6 mr. The discrepancy on this final pass is due entirely to the mistakes in the LGC coding; when the LGC coding is patched to correct the effect of the mistakes, the discrepancy becomes zero, i.e. the prediction (□) coincides with the rotation increment (+).

This lower section of Fig. 5 also separates the individual contributions to guidance coordinate frame rotation. The circles display the rotation increment contributions due to landing site truncation, and the squares represent the combined effects of landing site truncation and cross-range velocity. In this simulation, the contributions are about equal except the cross-range velocity becomes dominant near the close of P64. The truncation contributions were computed by dividing the truncation error by the current range. The cross-range velocity contributions were computed by averaging the Y components of velocity in guidance coordinates at the start and finish of the current guidance cycle, multiplying by the 2 second guidance period, and dividing by the current range. The maximum prediction error, (X) - (□), is under 1 mr and corresponds to under 1 bit error in position.

The final Figs, 6A thru 12C, display the yaw response to seven redesignation situations for each of three program configurations. The redesignation situations are defined on the figures and the three program configurations are as follows:

A. The LGC is patched to cause the apparent GAINAPPR to be close to unity on the final P64 pass. This aggravates the program mistake to the maximum extent. This was done in such a way as to avoid any other effect on the run. For those who are familiar with LGC coding, this effect was achieved by replacing JAPFG* +1 by POSMAX <u>after its final use in computing TTF/8.</u>

B. Displays unmodified Apollo 14 behavior.

C. The LGC erasables are modified to prevent guidance coordinate frame erection the final two passes of P64. This is done by loading TCGFBRAK with 77776 and TCGFAPPR with 1D 14 E+02 B-17 = 1O 00257.

The dots of Figures 6A thru 12C represent the autopilot's desired yaw gimbal angle CDUXD at two second intervals. These figures show that the maximum spurious yaw produced by the mistakes in the program using either the Apollo 14 erasables or unity apparent GAINAPPR was about 5°. However, the behavior under the three configurations was markedly different in every case, and the behavior was generally worst with unity apparent GAINAPPR.

HALVING THE MAXIMUM LANDING SITE TRUNCATION ERROR

It appears that the maximum truncation error could be cut in half by doubling the magnitude of the landing site radius (LAND) before multiplying by the semi-unit vector in the direction of the updated landing site. This would have to be done two places; in the computations following TTFINCR and in those following REDES1. In addition it would have to be demonstrated that the redesignation equations could never contribute to the truncation error when no redesignation was made, or else, if this could not be demonstrated, the redesignation equations could be skipped in cases of zero redesignation.

Considering that the yaw bias seems to work out at about 2° for Apollo 14 with a .059 m truncation error per pass, the maximum truncation error of .125 m would probably produce about 4° yaw bias. Is fixing the program worth the effort?

CONCLUSIONS

The mistakes found in the program should certainly be corrected for Apollo 15 as there is no guarantee we will be as lucky with erasables as we are on Apollo 14. Guidance frame erection on the final pass of P64 could be avoided on Apollo 14 or 15 by reloading TCGFBRAK with 77776, and there would be no other consequence. However, with the Apollo 14 erasables, the consequences of doing nothing are benign and that is our recommendation. The maximum landing site truncation error could be halved by the minor program change suggested herein, but it is doubtful that even this would be worth the effort. All other known sources of yaw rotation are normal.

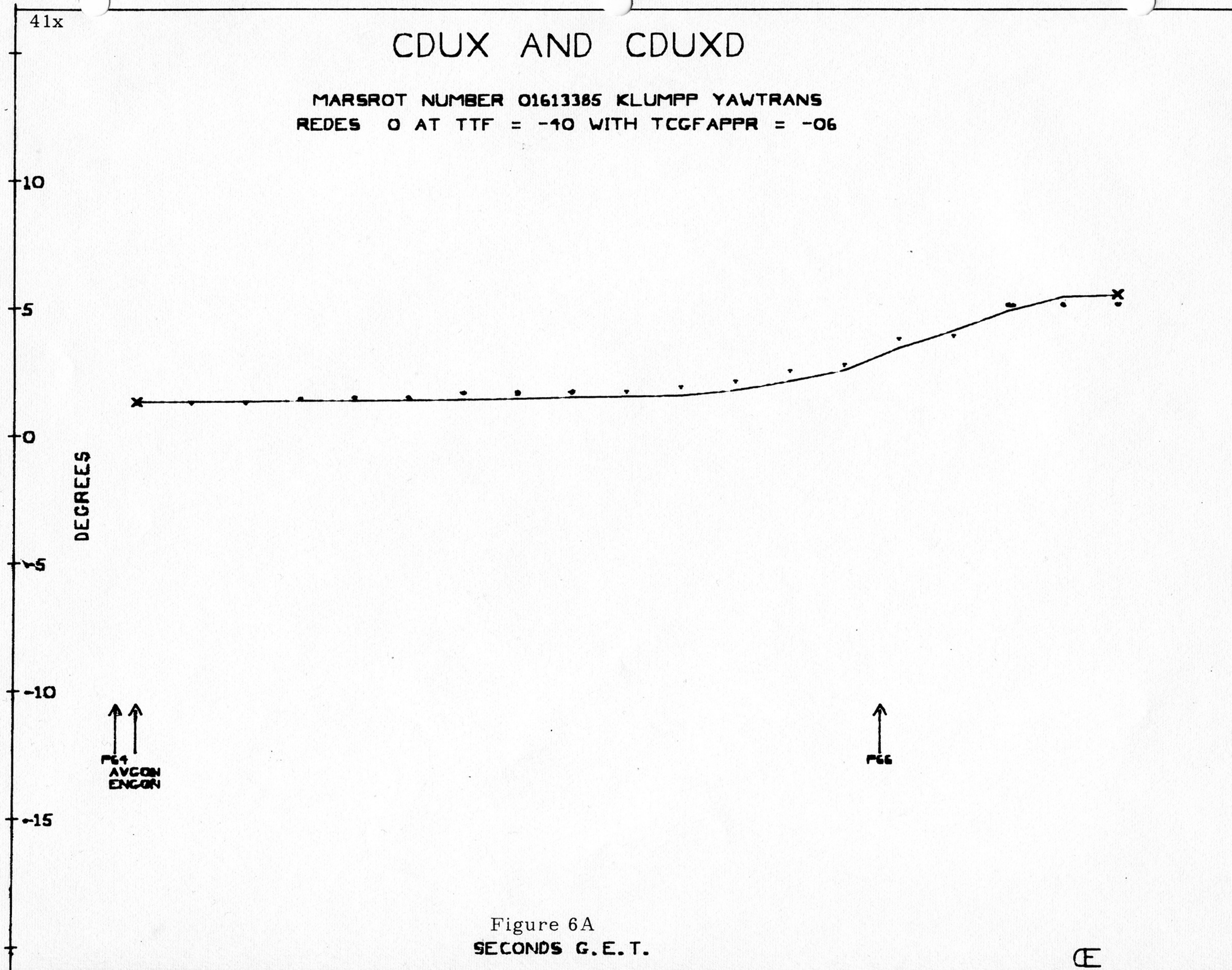
CDUX AND CDUXD
MARSROT NUMBER 01613385 KLUMPP YAWTRANS
REDES 0 AT TTF = -40 WITH TCGFAPPR = -06
10
5
0
-5
-10
-15
DEGREES
P64
AVCON
ENGON
P66
SECONDS G.E.T.

Figure 6A

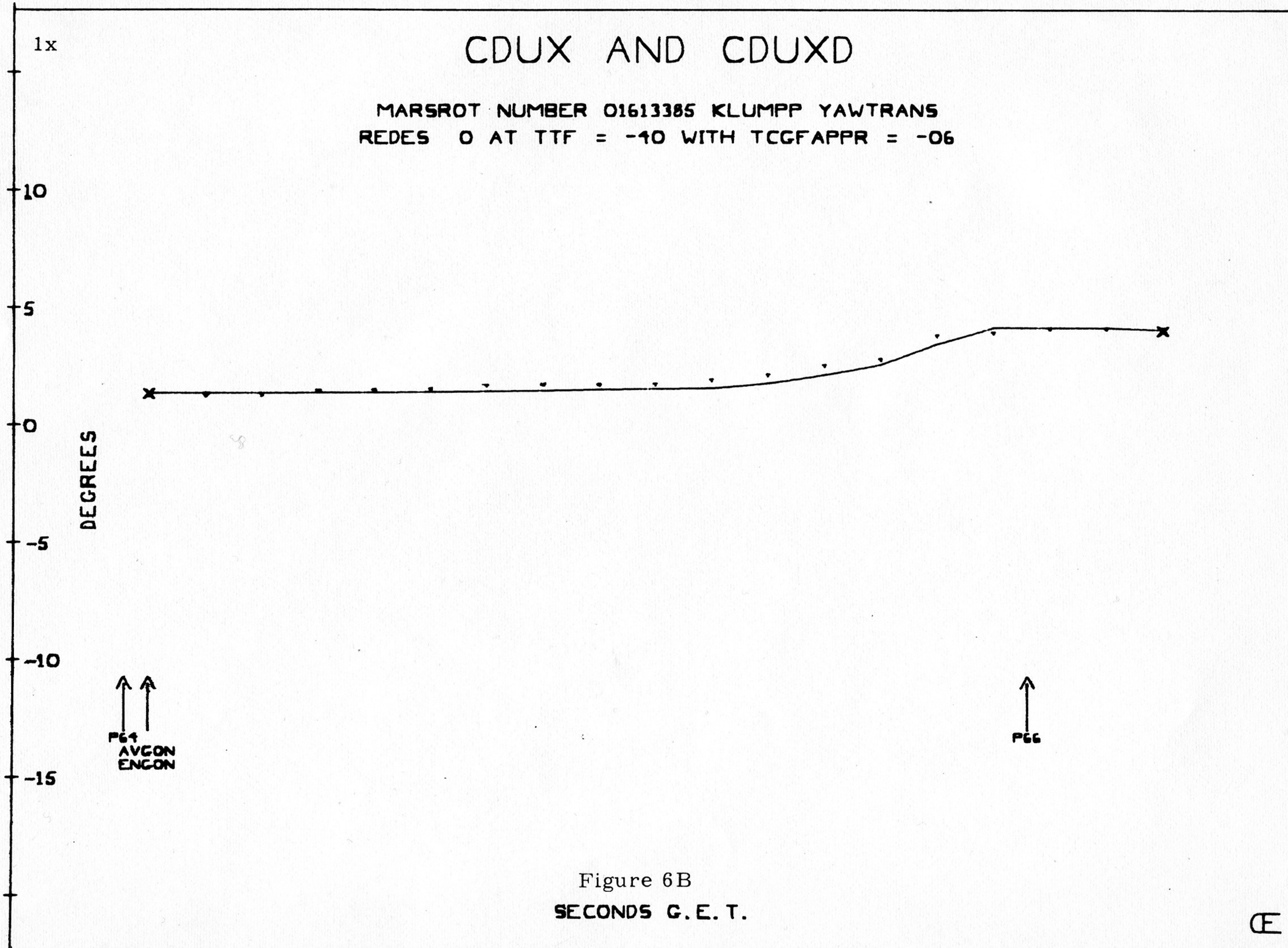
1x
CDUX AND CDUXD
MARSROT NUMBER 01613385 KLUMPP YAWTRANS
REDES 0 AT TTF = -40 WITH TCGFAPPR = -06
10
5
0
-5
-10
-15
DEGREES
P64
AVGON
ENGON
P66
SECONDS G.E.T.

Figure 6B

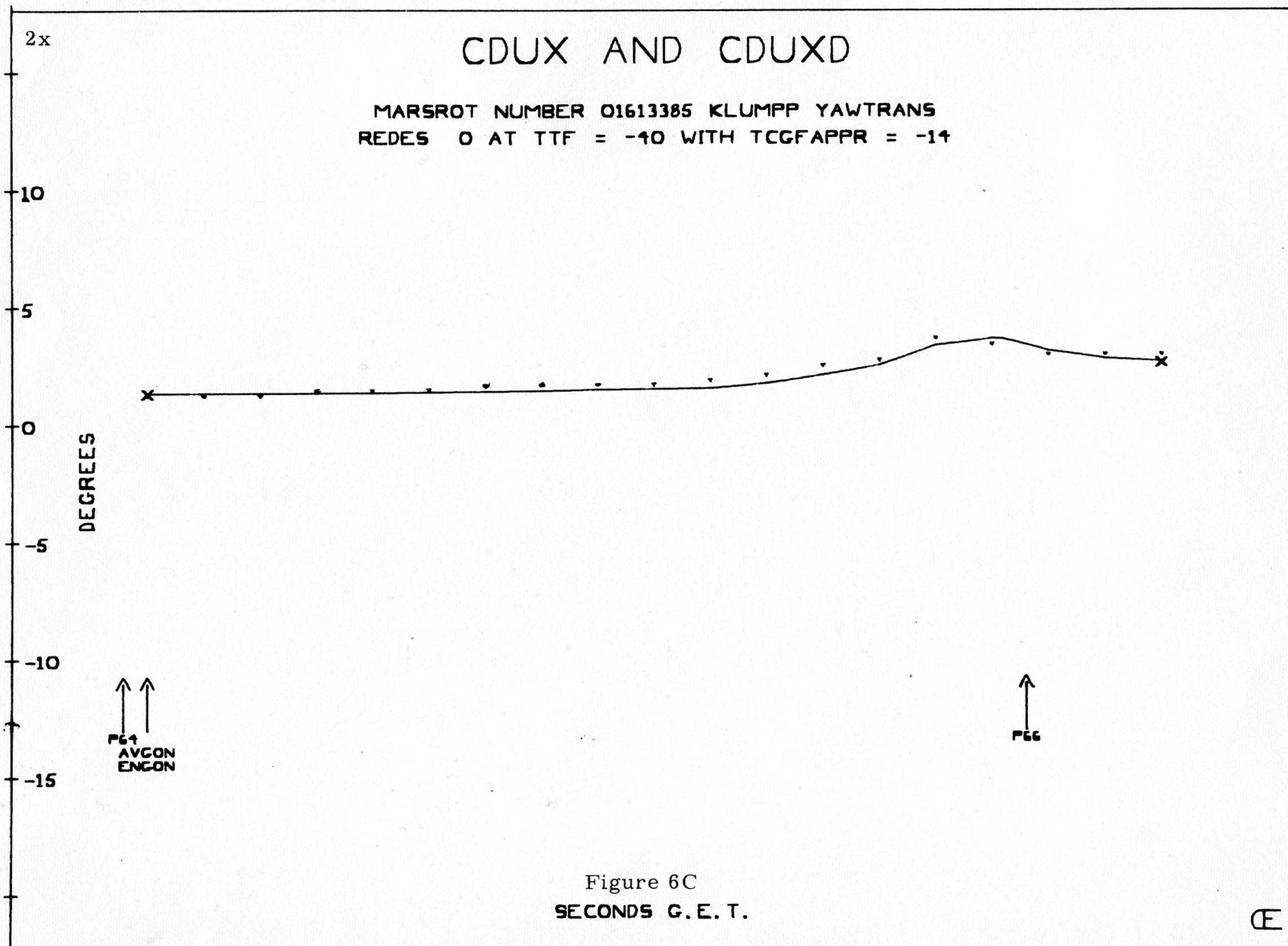
2x
CDUX AND CDUXD
MARSROT NUMBER 01613385 KLUMPP YAWTRANS
REDES 0 AT TTF = -40 WITH TCGFAPPR = -14
10
5
0
-5
-10
-15
DEGREES
P64
AVGON
ENGON
P66
SECONDS G.E.T.

Figure 6C

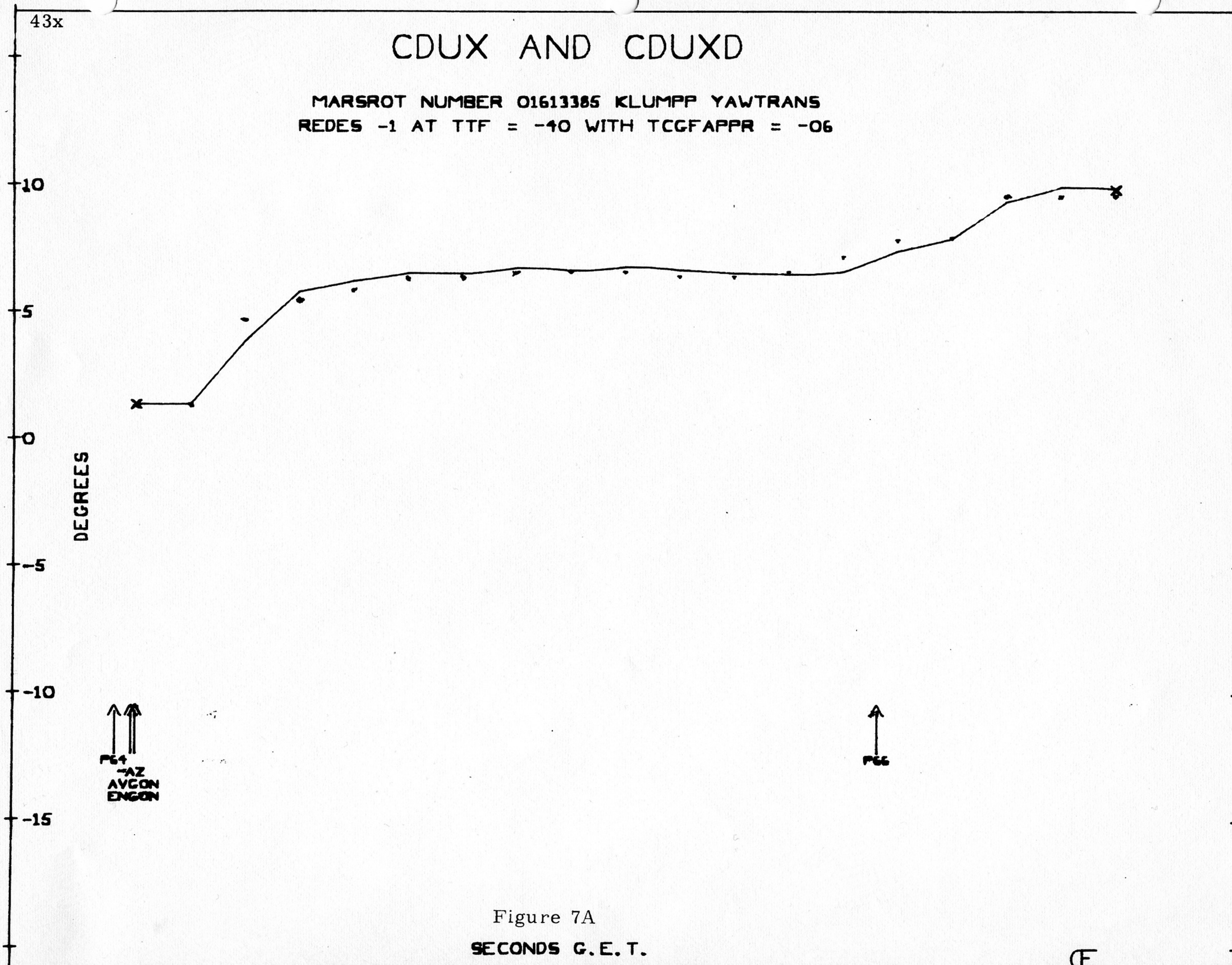
CDUX AND CDUXD
MARSROT NUMBER 01613385 KLUMPP YAWTRANS
REDES -1 AT TTF = -40 WITH TCGFAPPR = -06
10
5
0
-5
-10
-15
DEGREES
P64
-AZ
AVGON
ENGON
P66
SECONDS G.E.T.

Figure 7A

3x

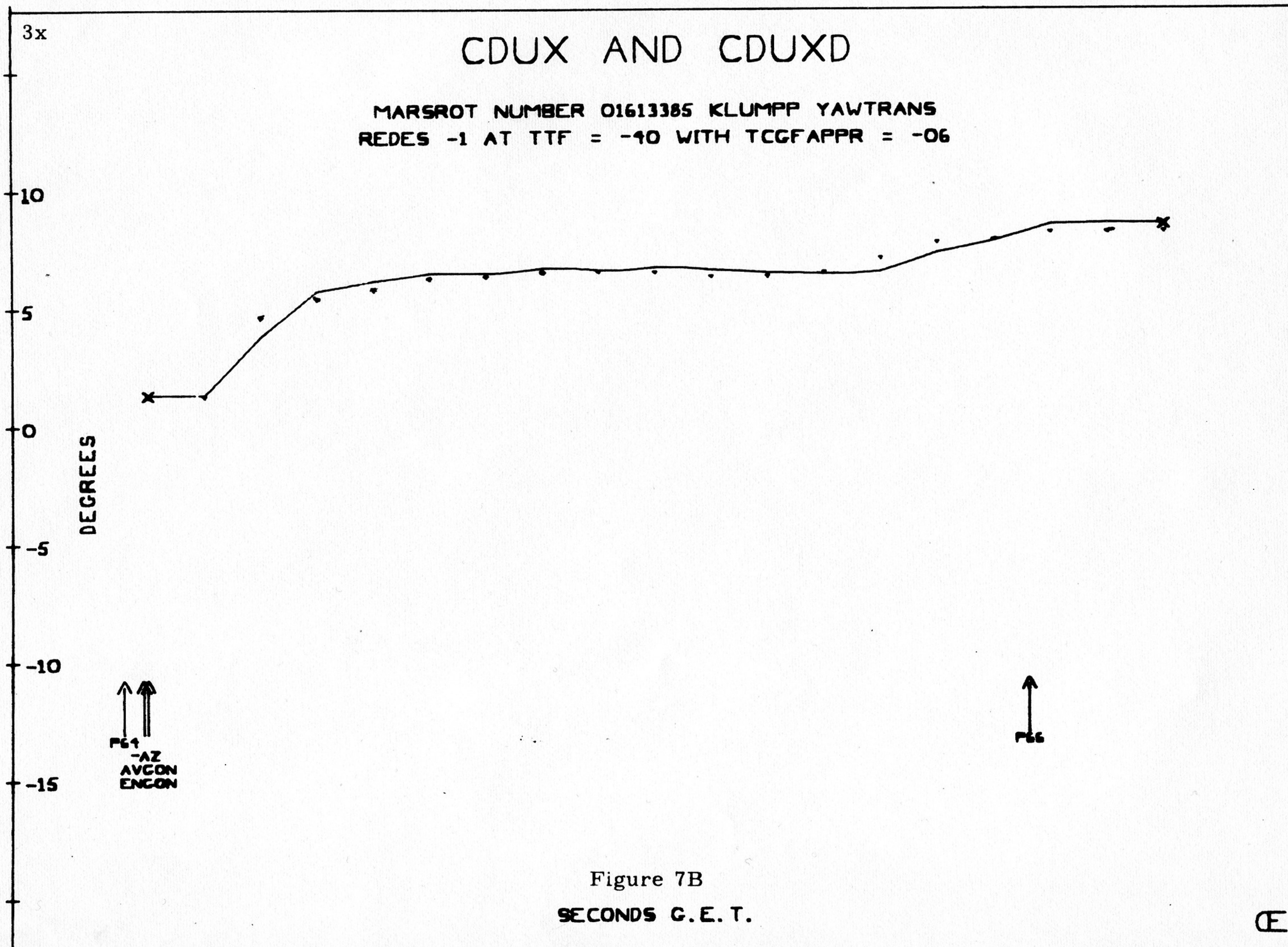
CDUX AND CDUXD
MARSROT NUMBER 01613385 KLUMPP YAWTRANS
REDES -1 AT TTF = -40 WITH TCGFAPPR = -06
10
5
0
-5
-10
-15
DEGREES
P64
-AZ
AVCON
ENGON
P66
SECONDS G.E.T.

Figure 7B

4x

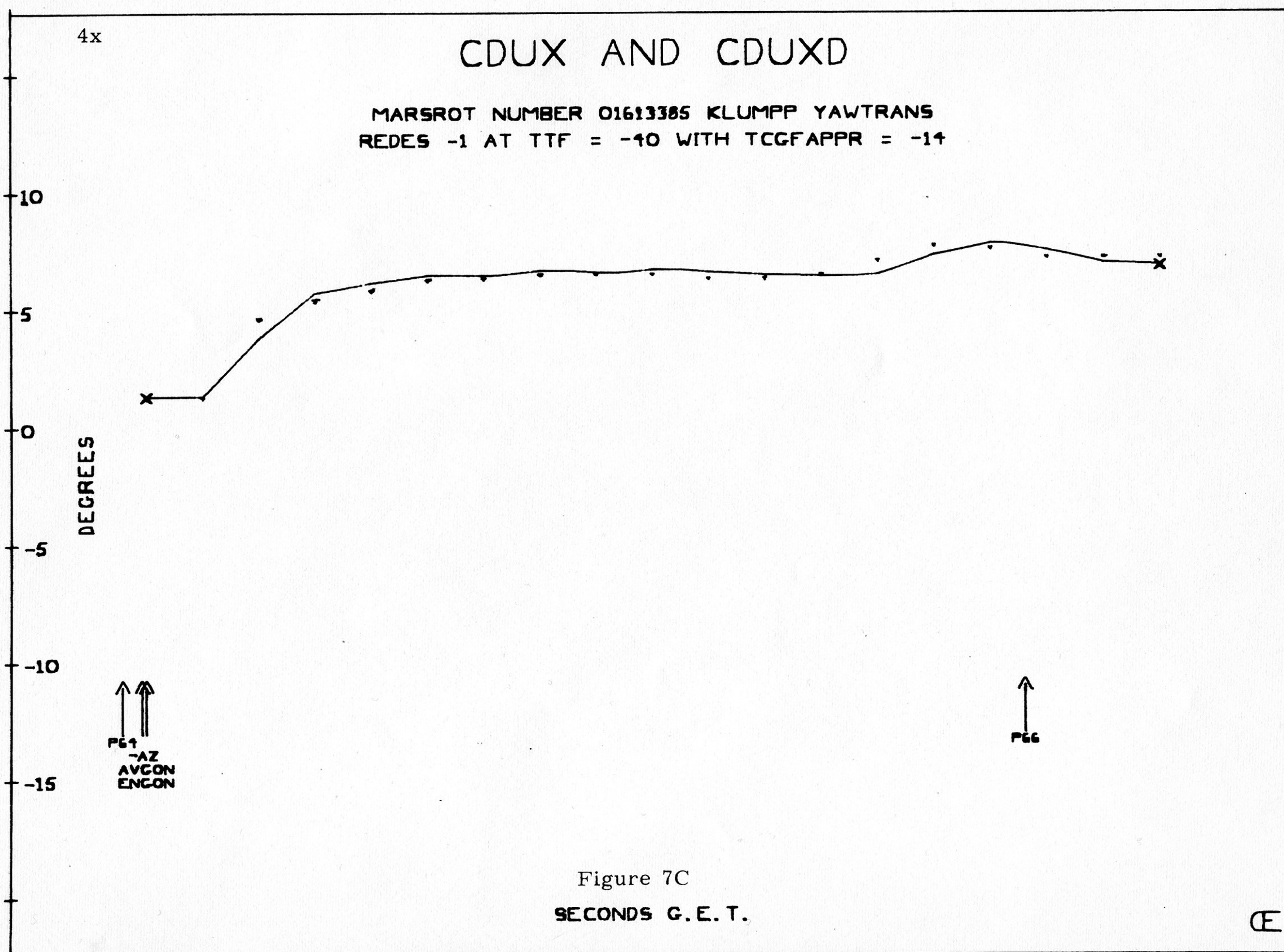
CDUX AND CDUXD
MARSROT NUMBER 01613385 KLUMPP YAWTRANS
REDES -1 AT TTF = -40 WITH TCGFAPPR = -14
10
5
0
-5
-10
-15
DEGREES
P64
-AZ
AVCON
ENCON
P66
SECONDS G.E.T.

Figure 7C

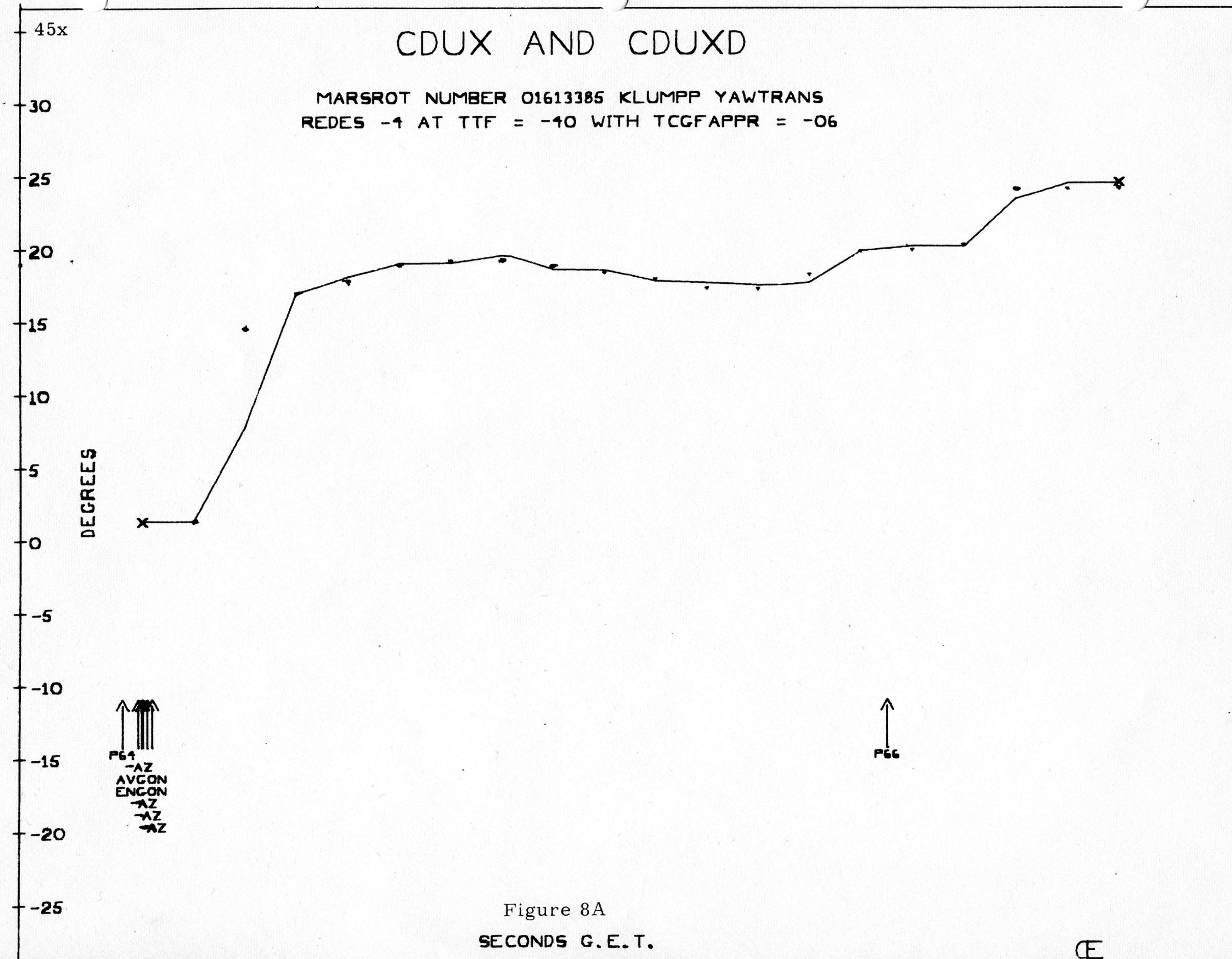
45x
CDUX AND CDUXD
MARSROT NUMBER 01613385 KLUMPP YAWTRANS
REDES -4 AT TTF = -40 WITH TCGFAPPR = -06
30
25
20
15
10
5
0
-5
-10
-15
-20
-25
DEGREES
P64
-AZ
AVGON
ENGON
-AZ
-AZ
-AZ
P66
SECONDS G.E.T.

Figure 8A

Œ

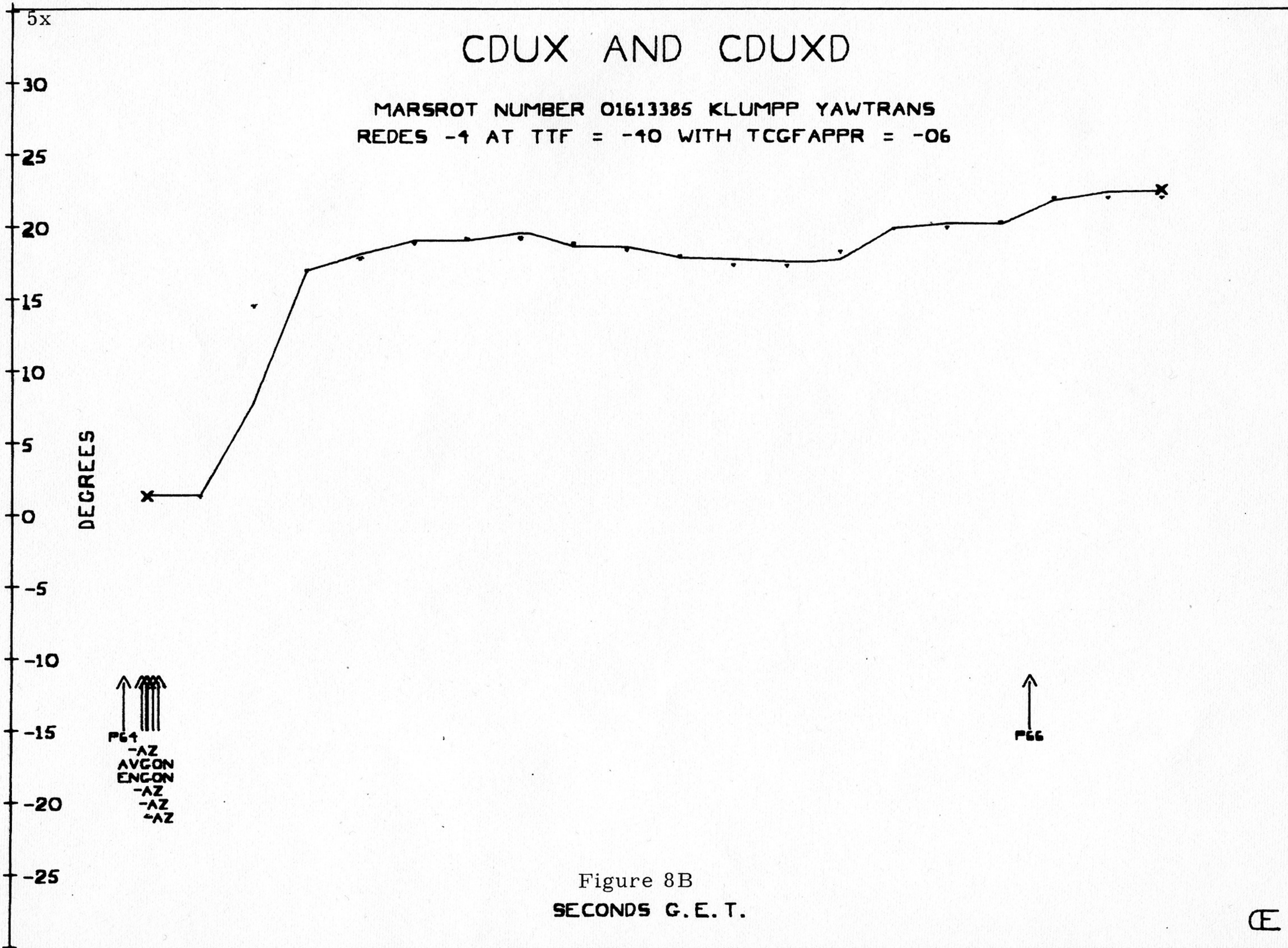
5x
CDUX AND CDUXD
MARSROT NUMBER 01613385 KLUMPP YAWTRANS
REDES -4 AT TTF = -40 WITH TCGFAPPR = -06
30
25
20
15
10
5
0
-5
-10
-15
-20
-25
DEGREES
P64
-AZ
AVGON
ENGON
-AZ
-AZ
-AZ
P66
SECONDS G.E.T.

Figure 8B

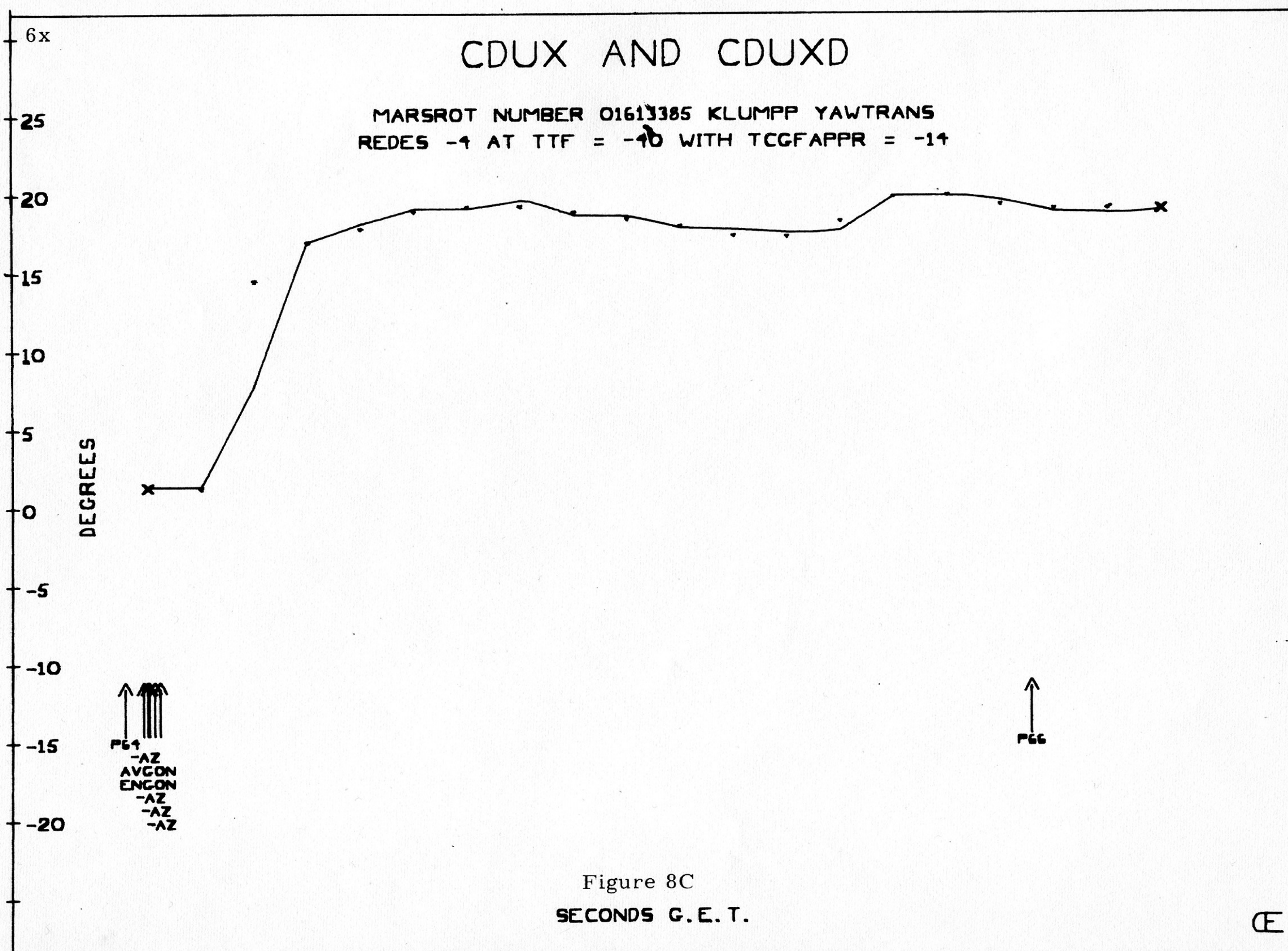
6x
CDUX AND CDUXD
MARSROT NUMBER 01613385 KLUMPP YAWTRANS
REDES -4 AT TTF = -10 WITH TCGFAPPR = -14
25
20
15
10
5
0
-5
-10
-15
-20
DEGREES
P64
-AZ
AVGON
ENGON
-AZ
-AZ
-AZ
P66
SECONDS G.E.T.

Figure 8C

47x

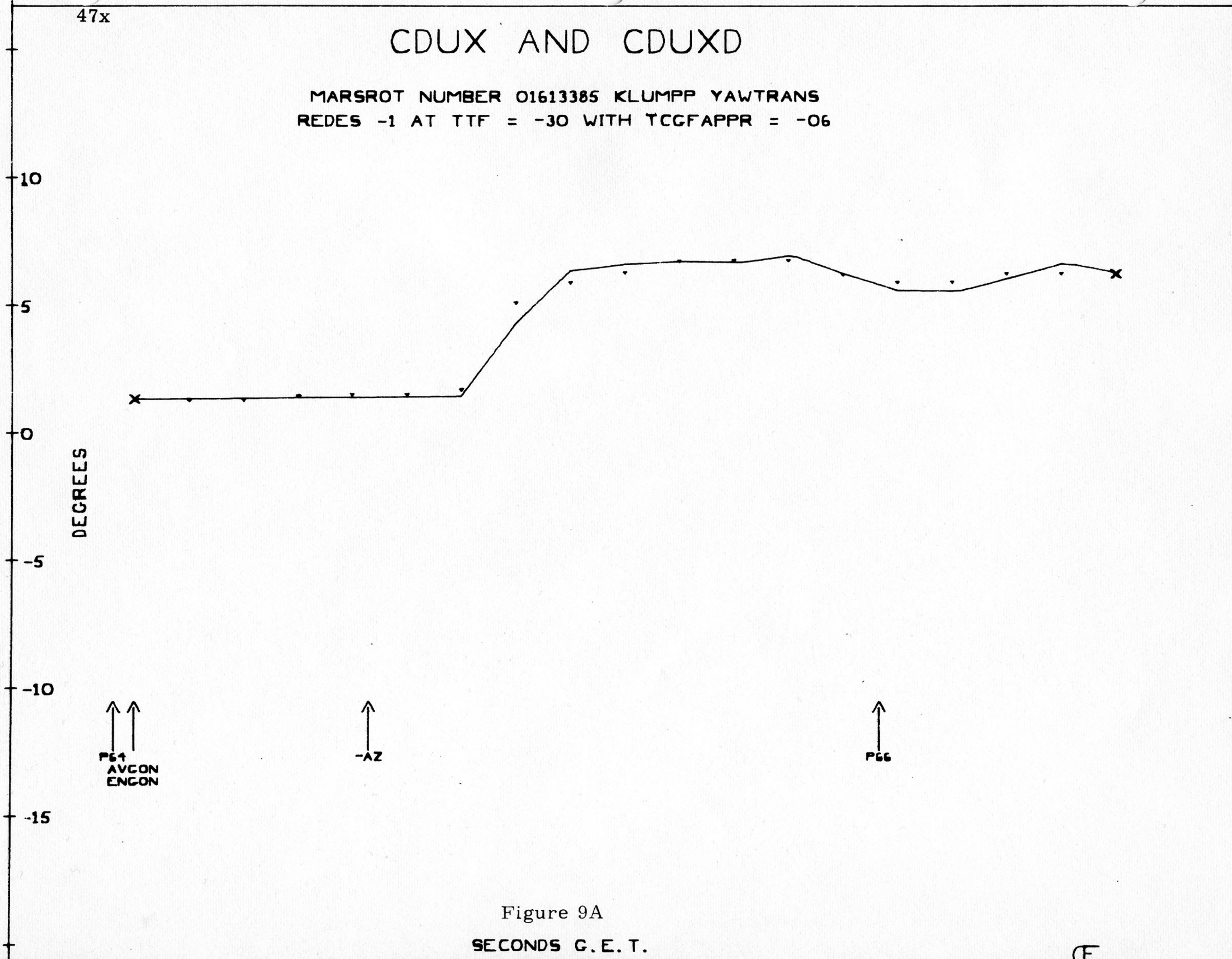

Figure 9A

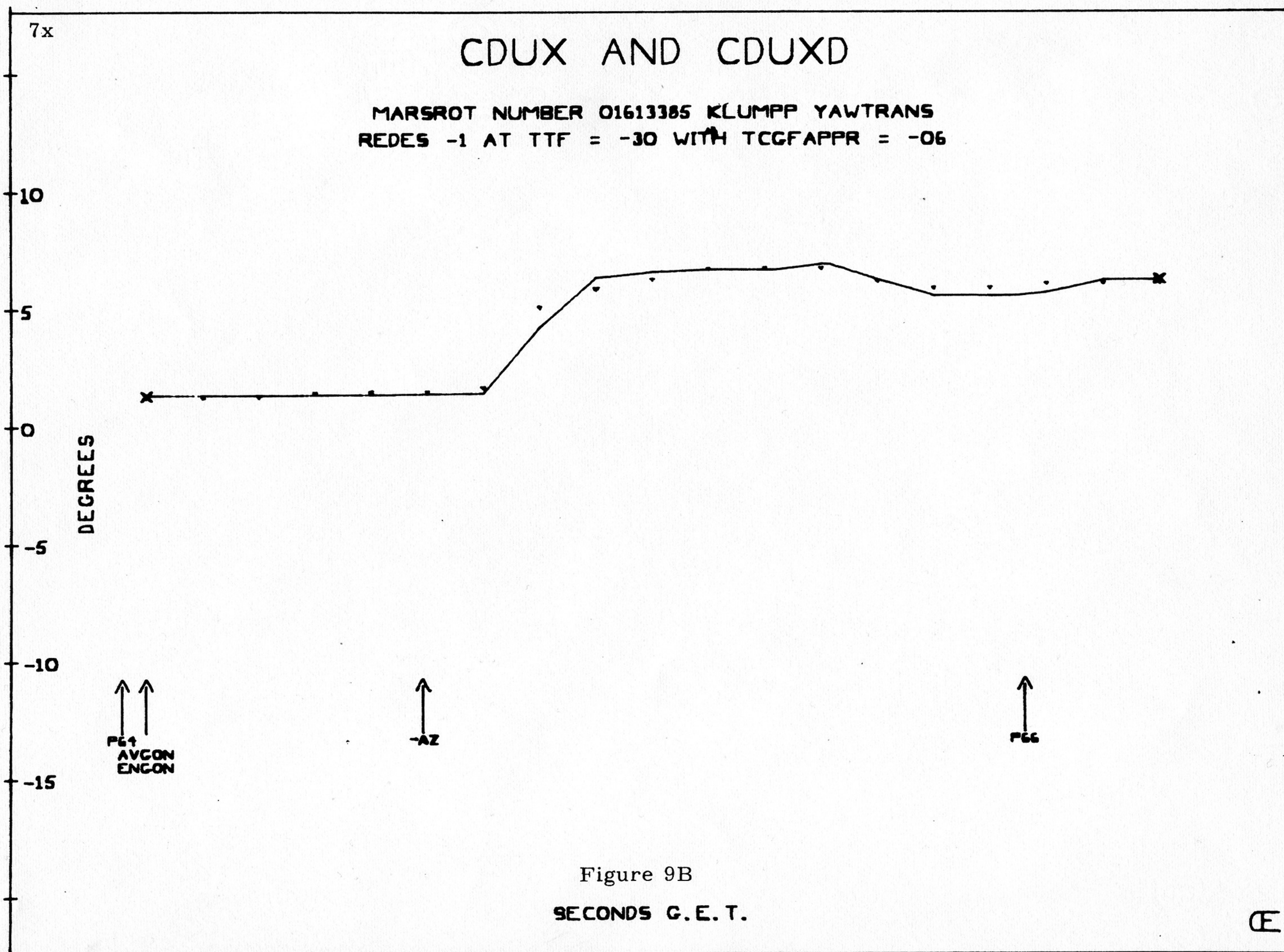

7x
CDUX AND CDUXD
MARSROT NUMBER 01613385 KLUMPP YAWTRANS
REDES -1 AT TTF = -30 WITH TCGFAPPR = -06
10
5
0
-5
-10
-15
DEGREES
P64
AVGON
ENGON
-AZ
P66
SECONDS G.E.T.

Figure 9B

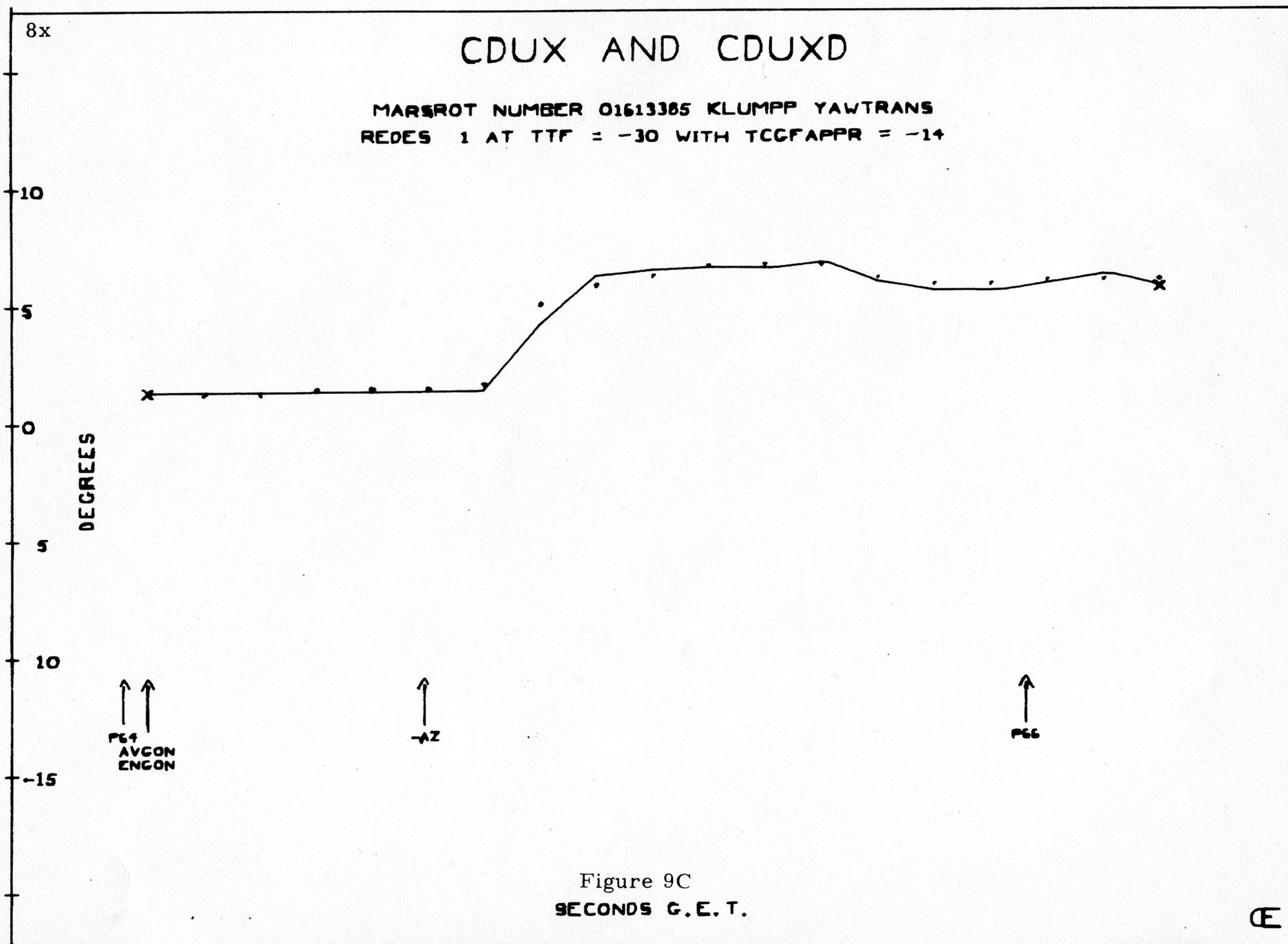
8x
CDUX AND CDUXD
MARSROT NUMBER 01613385 KLUMPP YAWTRANS
REDES 1 AT TTF = -30 WITH TCGFAPPR = -14
10
5
0
5
10
-15
DEGREES
P64
AVCON
ENGON
-AZ
P66
SECONDS G.E.T.

Figure 9C

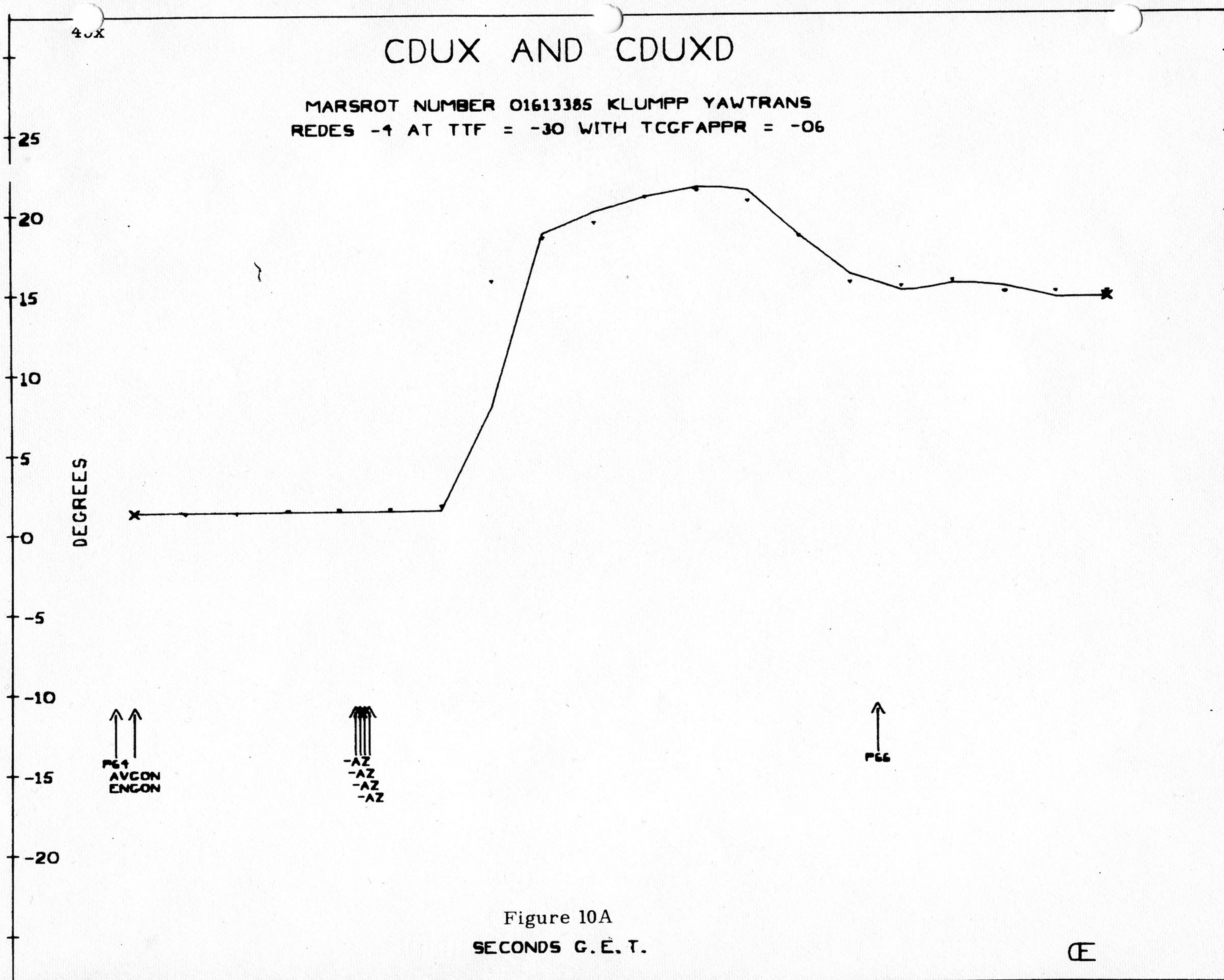
CDUX AND CDUXD
MARSROT NUMBER 01613385 KLUMPP YAWTRANS
REDES -4 AT TTF = -30 WITH TCGFAPPR = -06
25
20
15
10
5
0
-5
-10
-15
-20
DEGREES
P64
AVCON
ENGON
-AZ
-AZ
-AZ
-AZ
P66
SECONDS G.E.T.

Figure 10A

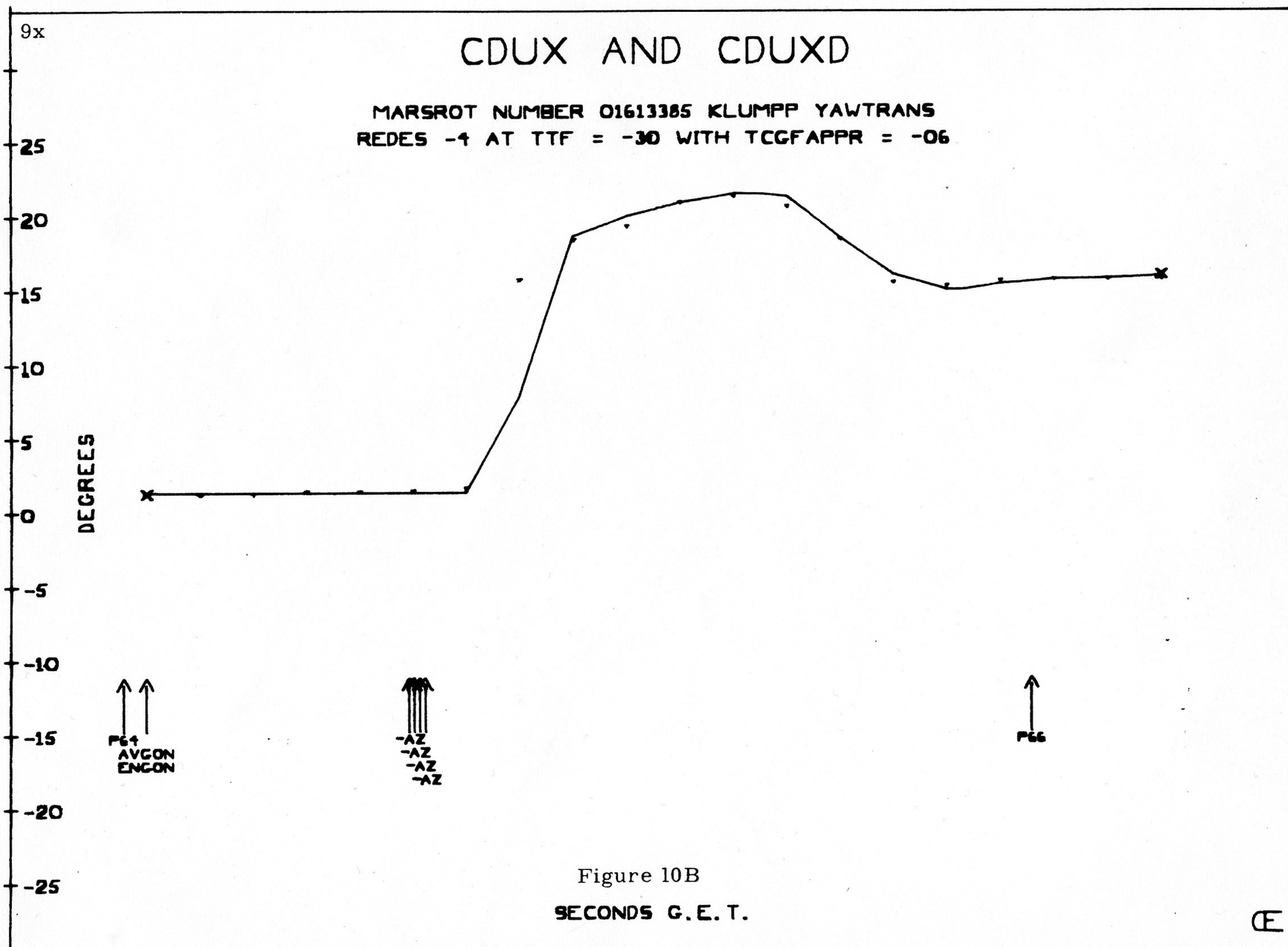
CDUX AND CDUXD
MARSROT NUMBER 01613385 KLUMPP YAWTRANS
REDES -4 AT TTF = -30 WITH TCGFAPPR = -06
25
20
15
10
5
0
-5
-10
-15
-20
-25
DEGREES
P64
AVGON
ENGON
-AZ
-AZ
-AZ
-AZ
P66
SECONDS G.E.T.

Figure 10B

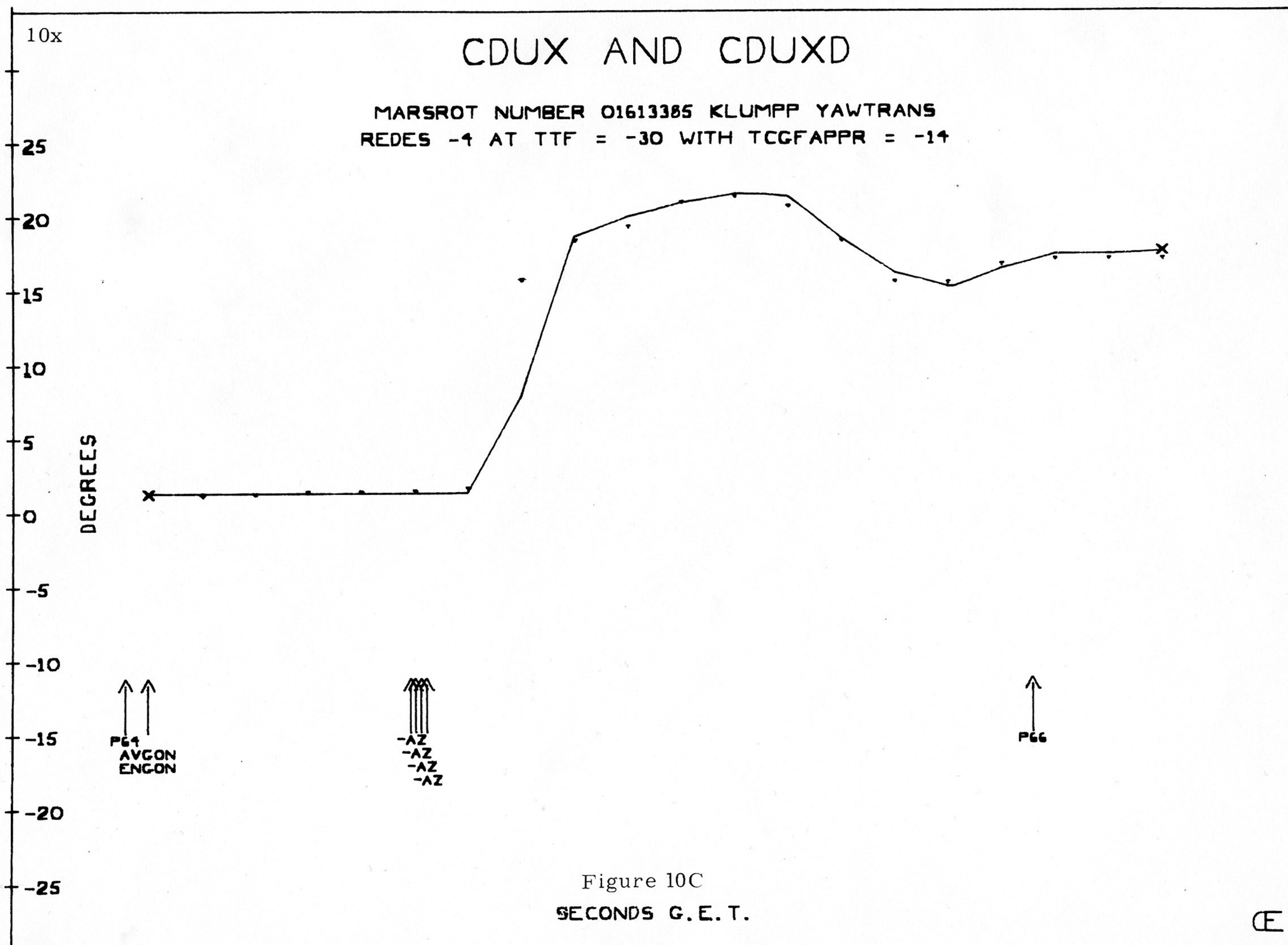
10x
CDUX AND CDUXD
MARSROT NUMBER 01613385 KLUMPP YAWTRANS
REDES -4 AT TTF = -30 WITH TCGFAPPR = -14
25
20
15
10
5
0
-5
-10
-15
-20
-25
DEGREES
P64
AVGON
ENGON
-AZ
-AZ
-AZ
-AZ
P66
SECONDS G.E.T.

Figure 10C

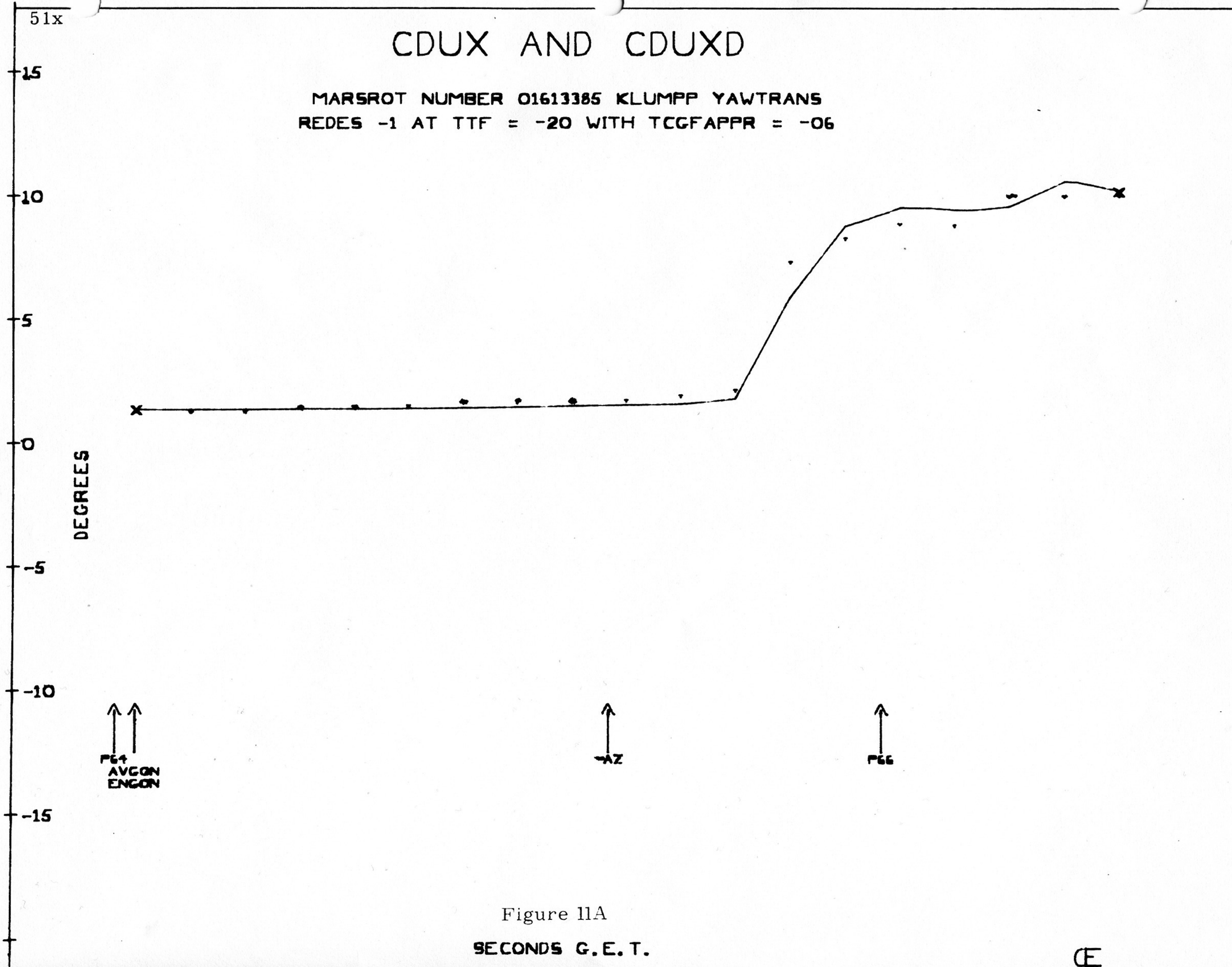
CDUX AND CDUXD
MARSROT NUMBER 01613385 KLUMPP YAWTRANS
REDES -1 AT TTF = -20 WITH TCGFAPPR = -06
15
10
5
0
-5
-10
-15
DEGREES
P64
AVGON
ENGON
AZ
P66
SECONDS G.E.T.

Figure 11A

11x

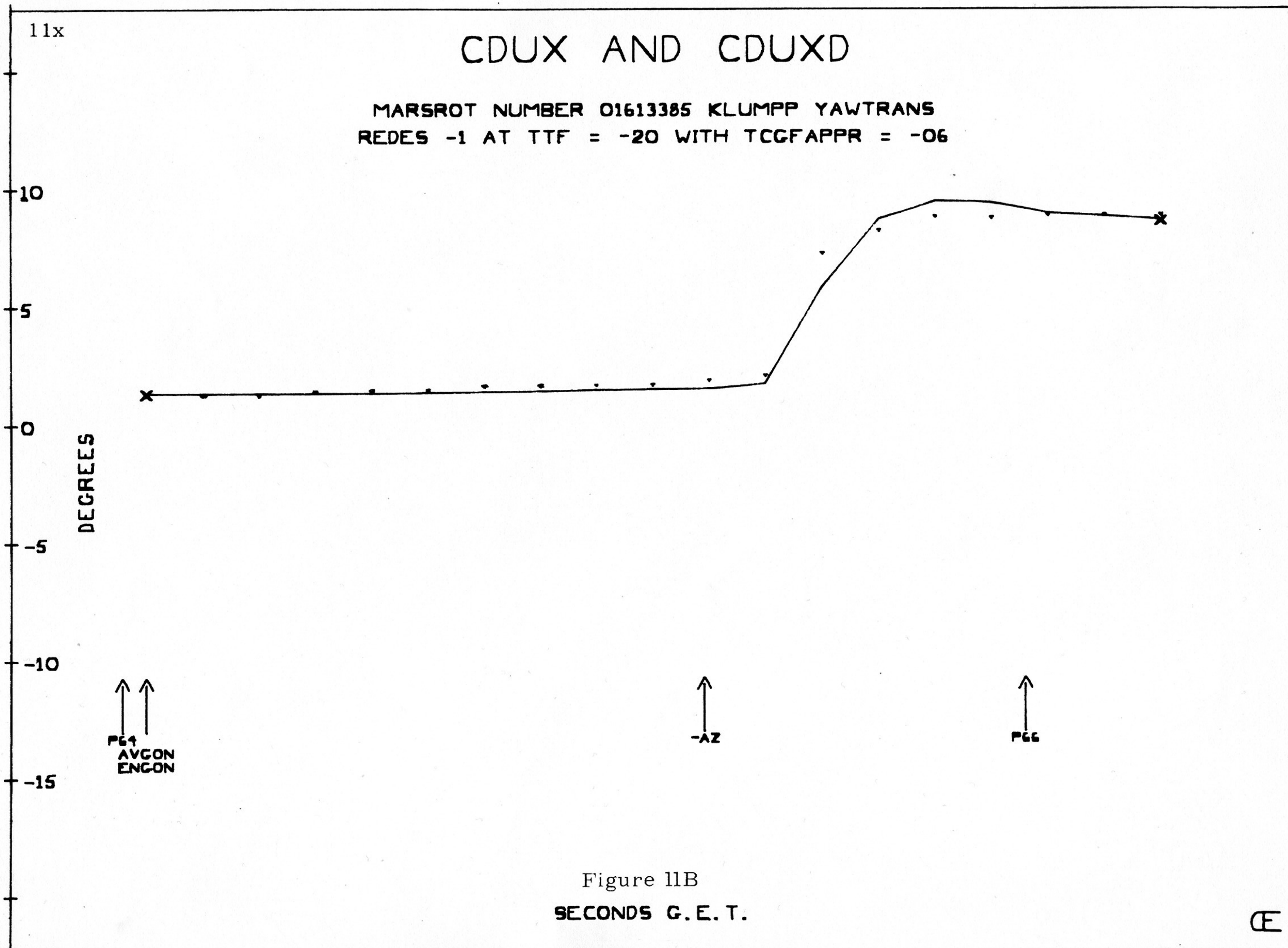

Figure 11B

12x

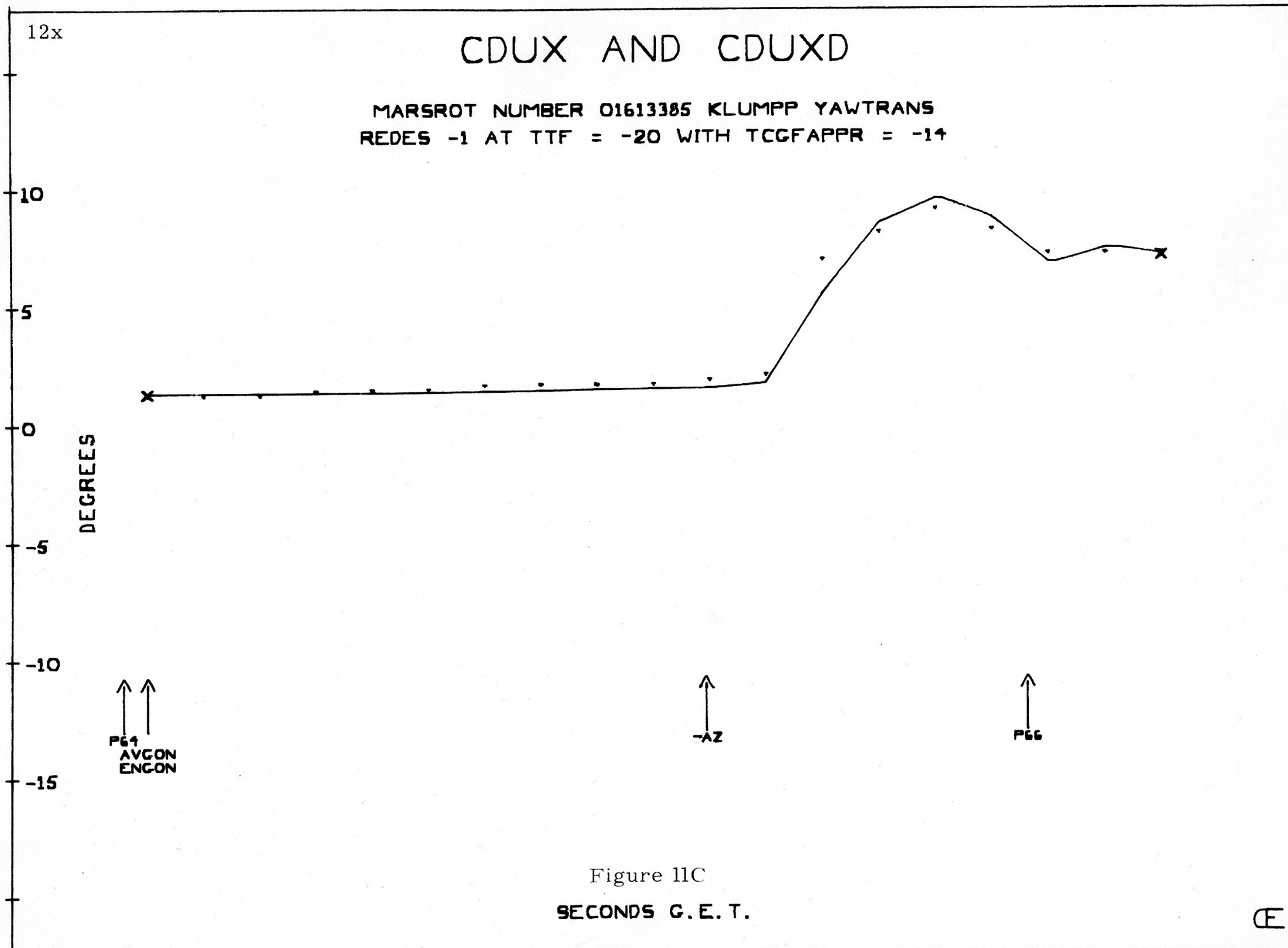

Figure 11C

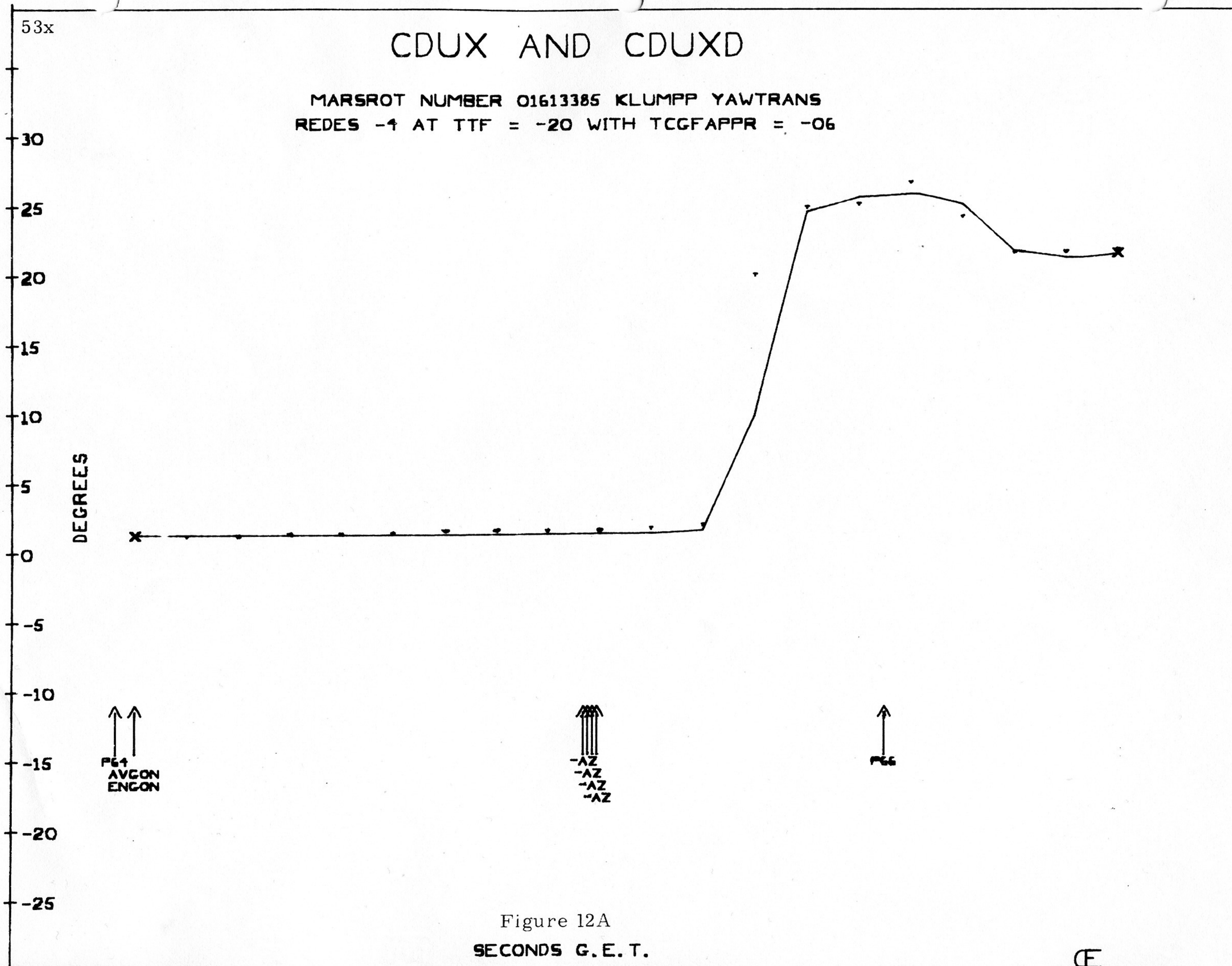
CDUX AND CDUXD
MARSROT NUMBER 01613385 KLUMPP YAWTRANS
REDES -4 AT TTF = -20 WITH TCGFAPPR = -06
30
25
20
15
10
5
0
-5
-10
-15
-20
-25
DEGREES
P64
AVGON
ENGON
-AZ
-AZ
-AZ
-AZ
P66
SECONDS G.E.T.

Figure 12A

13x

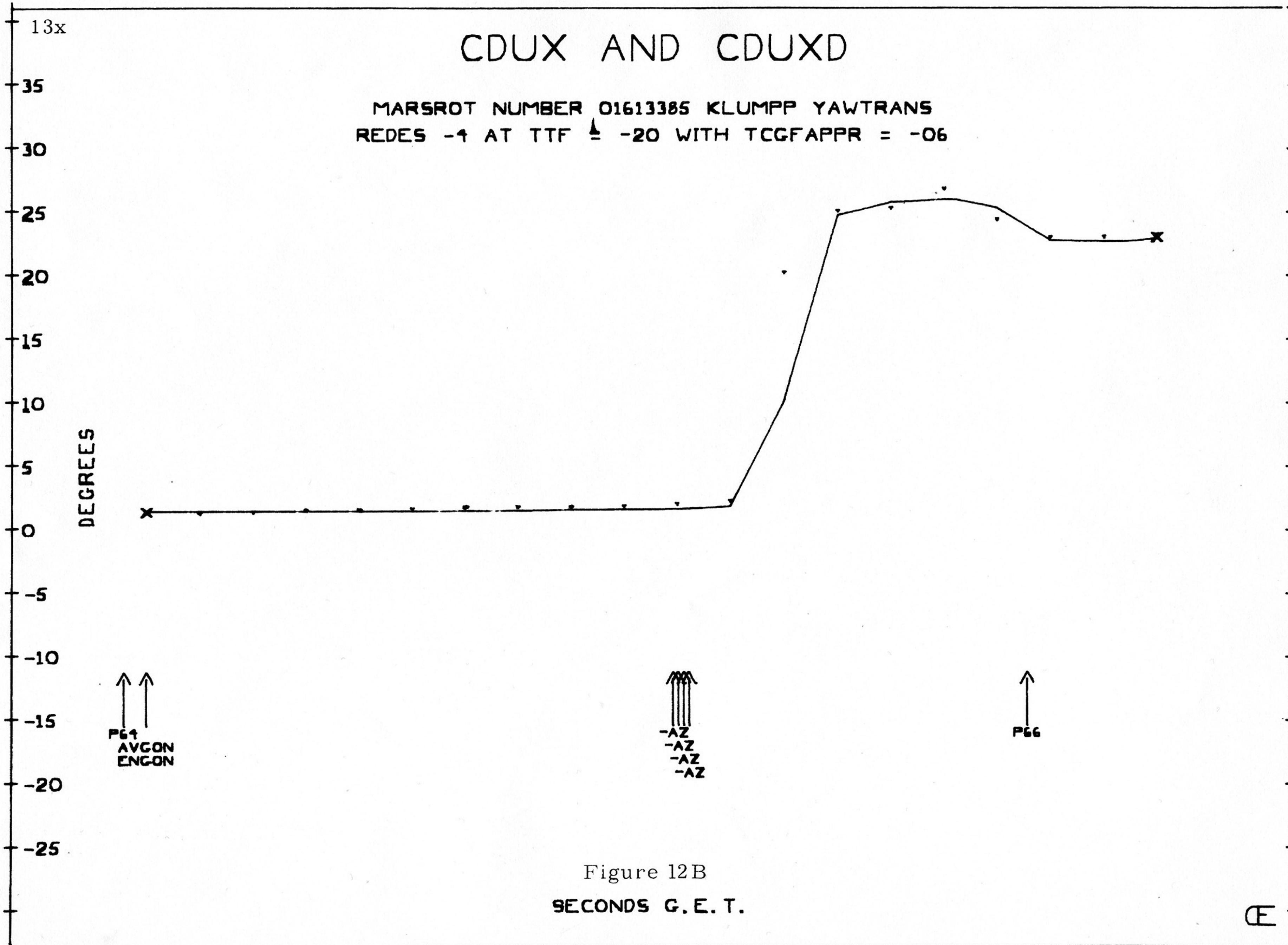

Figure 12B

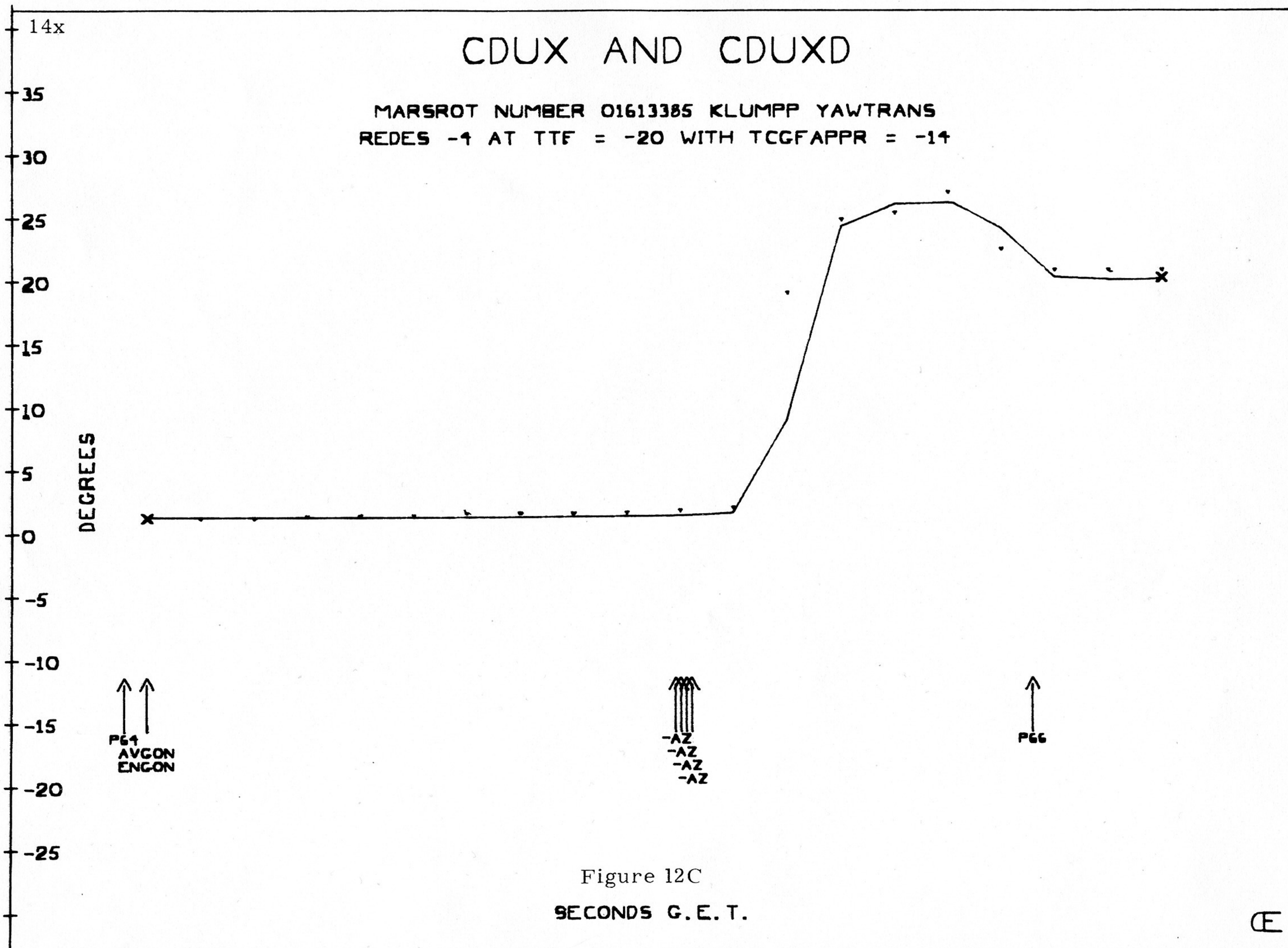
14x
CDUX AND CDUXD
MARSROT NUMBER 01613385 KLUMPP YAWTRANS
REDES -4 AT TTF = -20 WITH TCGFAPPR = -14
35
30
25
20
15
10
5
0
-5
-10
-15
-20
-25
DEGREES
P64
AVGON
ENGON
-AZ
-AZ
-AZ
-AZ
P66
SECONDS G.E.T.

Figure 12C

REFERENCES

1. Klumpp, Allan Memo to R. Larson, "Anomalies in Appllo 14 Descent", January 12, 1971.

2. Klumpp, A. R., "A Manually Retargeted Automatic Landing System for LM", MIT Instrumentation Laboratory, R-539 Rev. 1, August, 1967.

3. Klumpp, A., "FINDCDUW-Guidance Autopilot Interface Routine", Luminary Memo #27., Rev. 1, September 26, 1968.

4. Hull, L., "The Two Degree Yaw at the end of P64", Systems Engineering Memorandum SE-71-10, Delco Electronics Division of General Motors, Milwaukee, Wisconsin, 12, January 1971.

5. Klumpp, A., MIT/IL Software Anomaly Report, L-1D-23, Luminary, Rev. 178, 71-01-19.